Check for updates

Silico-Aluminophosphate and Alkali-Aluminosilicate Geopolymers: A Comparative Review

Yan-Shuai Wang, Yazan Alrefaei and Jian-Guo Dai*

*Department of Civil and Environmental Engineering, The Hong Kong Polytechnic University, Hong Kong, Hong Kong*

Chemically activated materials (often termed as geopolymer) have received attracting attentions in civil, material and environmental research fields as a toolkit alternative to traditional Portland cement in specific applications. This paper presents a comparative review on silico-aluminophosphate (SAP) geopolymers in terms of definition, chemistries involved during geopolymerization, mechanical performance, durability, environmental impacts, and their potentials in applications relative to conventional alkali-aluminosilicate (AAS) geopolymers. Recommendations for future applications are also highlighted. It is found that S-A-P gels with six-coordinated aluminum environment dominate in SAP geopolymers, while the aluminum in N-A-S-H gels formed in the AAS geopolymers is characterized by four-coordinated features. Besides, the slow performance development of SAP geopolymer matrix under ambient temperature curing can be compensated through incorporating additional countermeasures (e.g., metal sources) which allow the tailored design of such geopolymers for certain *in-situ* applications. Generally, the calcium-bearing C-(A)-S-H gels co-existing with N-A-S-H gels are dominant in AAS geopolymers, while the S-A-P gels enhanced by phosphate-containing crystalline/amorphous phases are the main products in SAP geopolymers. The SAP geopolymers show their environmental friendliness relative to the AAS geopolymers due to the utilization of phosphate activators that require lower production energy relative to silicate-containing activators. However, the higher cost of phosphate activators may confine the applications of SAP geopolymers in some exquisite or special fields.

Keywords: silico-aluminophosphate, alkali-aluminosilicate, geopolymerization mechanism, environmental impacts, sustainable development

GENERAL ABOUT CEMENT AND GEOPOLYMER BINDERS

Cement, routinely denoted as ordinary Portland cement (OPC), is described as a cohesive material that can set and bind sands and gravels together; such binder is excessively used to prop up the modern urban agglomerations (Taylor, 1997; Neville, 2011; Shi et al., 2011). However, the annual huge consumption of contemporary cement has caused several environmental issues worldwide due to the high carbon footprint (e.g., the inescapable decarbonation of limestone) during cement production. Geopolymer binders, characterized by higher durability and greenness relative to the conventional OPC, have gained many attentions recently as a promising partial substitute to OPC (Provis and Bernal, 2014; Provis et al., 2015).

Initially, the geopolymer was strictly defined as the alkali-activation of raw aluminosilicates (e.g., metakaolin as a precursor) without (or with little) other components (i.e., Ca, Mg, etc.) (Davidovits, 2011). The geopolymer formation can be described as a polymer-like condensation process (as shown in Equation 1) where the loss of water between two hydroxyl groups occurs in inorganic materials (Wilson and Nicholson, 2005; Davidovits, 2011). Such chemistry is also extended to the reaction between two different hydroxyl-containing groups, e.g., the isolated aluminate (IV) and silicate (IV) units to reconstruct connected gels with chain or ring network structure through condensation chemistry in alkali-activated aluminosilicate binders, as shown in Equation (2) (De Jong et al., 1983). Thus, such high-connectivity molecular structures of the formed products can perform excellently in terms of strength and durability (Walkley et al., 2017). Later on, the phosphate-activated aluminosilicate was developed and incorporated into the geopolymer category due to the similar condensation process (Liu et al., 2010; Davidovits, 2011; Guo et al., 2016; Wang et al., 2017, 2018b).
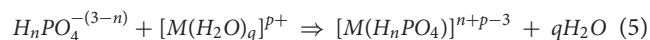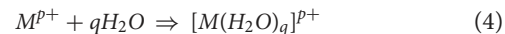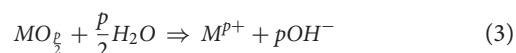
$$\equiv Q - OH + HO - Q \equiv \xrightarrow{Catalysis} \equiv Q - O - Q \equiv + H_2O \quad (1)$$
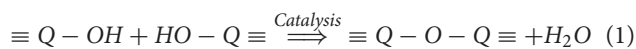
where, Q denotes the hydroxyl-containing group (e.g., orthosilicic group).

$$\equiv Si - OH + HO - Al \equiv \xrightarrow{Alkaline} \equiv Si - O - Al \equiv + H_2O \quad (2)$$

The catalytic activation process of un-doped aluminosilicate precursors is usually enhanced by external energies (e.g., heat, ultraviolet, and microwave), otherwise it requires a long hardening duration, depending on the reactivity of the aluminosilicate sources (Agarwal, 2006; Zhang et al., 2016). Such special curing methods are acceptable in precast geopolymer industry, yet very challenging to be implemented in *in-situ* constructional operations (Provis and Bernal, 2014). Therefore, it is imperative to develop other chemical processes for room-temperature hardening mechanism in geopolymers.

In alkali-activated systems, the calcium-containing solid aluminosilicate sources, such as ground granulated blast-furnace slag (GGBS) or high-calcium fly ash (FA), are habituated under high alkaline environment to form C-(A)-S-H gels rapidly (Wang et al., 1994; Shi and Qian, 2000; Li et al., 2010). It should be noted that the high volume of calcium species in FA (e.g., Class C) greatly influences the operating time of their corresponding binders due to their flash setting, which needs to be overcome by the use of retarding additives, e.g., sodium tetraborate (Nicholson et al., 2005; Tailby and MacKenzie, 2010). The C-(A)-S-H gel shows some similar features to that of C-S-H gel that is dominant in the conventional OPC cement. In the meantime, soluble silicates (sometimes mixed with aluminates) are generally introduced into the alkaline activating solution with the same aim of obtaining a rapid sol/gel transition (Benavent et al., 2016). Such actions provide the alkali-activated binders matrices with high efficiency in terms of mechanical performance and durability (Ding et al., 2016, 2018; Shang et al., 2018; Xue et al., 2018).

As a comparison, in phosphate-activated systems, some solid agents (e.g., alkali metals) can be incorporated into the aluminosilicate sources to induce an acid-base chemistry which generally facilitates the formation of crystalline (e.g., products in magnesium/calcium phosphate cement) or amorphous phosphate phases during the chemical activation of aluminosilicates (Wagh, 2016; Wang, 2018). Such acid-base chemistry can be described in Equations (3–5). Initially, the release of cations from the metal oxides occurs through hydrolysis reaction (shown in Equation 3), following, the metal cations react with water to form the aquo ions (hydration reaction in Equation 4). The polyacids generated by the acidic salt or acid (e.g., phosphate radicals) react with the aquo ions (e.g., $Mg[H_2O]_6^{2+}$) as described in Equation (5) (Ding et al., 2012). The whole conversion process from sols (i.e., colloidal solutions) to gels can be described as exothermic and rapid. Such fast acid-base chemistry can be used for possible improvements in the early performance of the phosphate activation of aluminosilicate.

$$MO_{\frac{p}{2}} + \frac{p}{2}H_2O \Rightarrow M^{p+} + pOH^- \quad (3)$$

$$M^{p+} + qH_2O \Rightarrow [M(H_2O)_q]^{p+} \quad (4)$$

$$H_nPO_4^{-(3-n)} + [M(H_2O)_q]^{p+} \Rightarrow [M(H_nPO_4)]^{n+p-3} + qH_2O \quad (5)$$

Due to the environmental concerns, the currently used aluminosilicate sources in the geopolymer production are usually industrial byproducts (e.g., FA and GGBS) rather than the materials available naturally (e.g., metakaolin [MK]) (Toniolo and Boccaccini, 2017). The MK [$2SiO_2 \cdot Al_2O_3$] is the product of the dehydroxylated clay mineral kaolinite [$Si_2O_5Al_2(OH)_4$] upon calcination under high temperature (Sperinck et al., 2011) to yield disordered aluminosilicates with Si-O-Al(1O) (i.e., Al in five-fold coordination) and Si-O-Al(2O) (i.e., Al in four-fold coordination), which is an ideal precursor for geopolymer preparation. Due to the limited availability of clay mineral and high temperature calcination that may cause undesirable high cost and energy consumption, the MK is still confined to laboratory use with the aim of investigating the mechanism of geopolymer formation (Khale and Chaudhary, 2007); however, the use of MK is recommended for some practical low-volume high-value applications (e.g., bioactive ceramics, electronic ceramics, drug delivery agents, etc.) (MacKenzie, 2015). On the other hand, the industrial raw materials (typically the byproducts of power stations like FA and iron & steel industries like GGBS) are chemically complex due to their diverse production technologies (Pacheco-Torgal et al., 2008; Yao et al., 2015; Xu and Shi, 2018). Thus, some "impurities" (the impurities mean different available components in the precursor other than aluminosilicates) in the byproducts will induce non-geopolymeric chemistries, thus the acidic or alkaline activators will generate different chemical compositions, crystallinities and phases. Accordingly, the formation process of the impurity-contained geopolymer (i.e., silico-aluminophosphate [SAP] geopolymer and alkali-aluminosilicate [AAS] geopolymer) can be illustrated based on the acidic and alkaline activation conditions as shown in **Figure 1**. In addition to the different pH conditions, the resulting

molecular structures of the SAP and AAM geopolymers vary to wide extent, especially the chemical environment of Al in the formed gels, which behaves as Al(VI) and Al(IV) in SAP geopolymer and AAS geopolymer, respectively. Such formation model and mechanism will be discussed in section Formation Model and Mechanism of Geopolymer.

Recently, the AAS geopolymers have been investigated from multiple angles, such as the synthesis mechanism and chemistry (Provis, 2013; Provis and Bernal, 2014; Provis et al., 2015), properties and durability (Bernal et al., 2014; Arbi et al., 2016; Ding et al., 2016), life cycle analysis (Habert et al., 2011; Ouellet-Plamondon and Habert, 2015), and multi-field applications (MacKenzie, 2015; Rao and Liu, 2015; Luukkonen et al., 2019). Yet, the available review related to the SAP geopolymer is limited even though such type of geopolymer was termed as aluminosilicate phosphate cement (Khabbouchi et al., 2017; Katsiki, 2019), phosphoric acid-based geopolymer (Liu et al., 2012; Guo et al., 2016), phosphate-based geopolymer (Wang et al., 2017), acid-based geopolymers (Mathivet et al., 2019), and phosphate-bonded materials (MacKenzie, 2015). This paper mainly reviews the development of the SAP geopolymers in reference with the conventional AAS geopolymers.

TERMINOLOGY AND CLASSIFICATION

The research era of alkali-activated materials (AAMs) started in 1908 (Kühl, 1908; Provis and Van Deventer, 2013), and since then AAMs were explained as cement-like materials formed by the reaction between an aluminosilicate precursor and an alkaline activator. Then, the tranquility was broken by the term "geopolymer" coined by Davidovits who inadvertently produced an inorganic polymer-like material with good fire-resistance (Davidovits, 2011). The traditional geopolymer was predominantly confined to the binder prepared by the aluminosilicate sources with marginal impurities. Such geopolymer binder mainly highlights the chemical behaviors of aluminate and silicate species, including bonds breaking (i.e., decomposition reaction) and remaking (i.e., polymerization reaction). Afterwards, the activation approach of aluminosilicate precursors was extended to phosphate species and termed as phosphate-based geopolymer (Wagh, 2004; Davidovits, 2011). The empirical formulas of the AAS and SAP geopolymers are shown in Equations (6, 7), respectively (Cui et al., 2008; Davidovits, 2011; Wagh, 2016).

$$M_n[-(SiO_2)_z - AlO_2]_n \cdot mH_2O \qquad (6)$$
$$[-(Si - O)_z - Al - O - P]_n \cdot mH_2O \qquad (7)$$
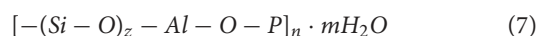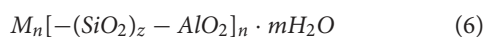
where n is the degree of geopolymerization, z is 1, 2, or 3, and M is an alkali cation (e.g., K or Na).

Recently, the term "chemically-activated materials" (CAMs) was also proposed to describe the aluminosilicate sources that can be activated to create cementitious matrices using some chemical solutions (e.g., alkali-silicate, phosphate and other chemicals) (CAM2017 International Conference, Gold Coast, Australia). However, the term "geopolymer" seems to be more attractive to (even widely-used by) engineers because such

term is more concise and easy-spreading. In this paper, all the binders primarily prepared by aluminosilicate materials and some chemical activators were named as modern geopolymer for the convenient circulation in academic, engineering and business communities. The modern geopolymers are further classified into two categories according to the activation approach: alkali-aluminosilicate (AAS) geopolymer and silico-aluminophosphate (SAP) geopolymer. The terminology and development of the geopolymers are summarized in **Figure 2**. In modern geopolymer, the AAS geopolymer denotes the alkali activation of aluminosilicate precursors such as the calcium-containing sources (e.g., alkali-activated GGBS binder), the low-impurity aluminosilicates (e.g., alkali-activated FA/MK binder), or their blends (e.g., alkali-activated GGBS/FA blends), while the SAP geopolymer implies that the aluminosilicate sources are pre-mixed with some metals and activated by the acid phosphate or other phosphates. It is good to mention that the activation methods assisted by external energies [e.g., microwave (Chindaprasirt et al., 2013a), autoclaved (Rashad et al., 2012), and mechanical activation (Kumar and Kumar, 2011)] are not involved in this review.

FORMATION MODEL AND MECHANISM OF GEOPOLYMER

AAS Geopolymer

As commonly explained, the three-dimensional network of alkali-aluminosilicate geopolymer is configured with the negative $[AlO_4]^{5-}$ and $[SiO_4]^{4-}$ tetrahedrons in addition to positive alkali metal ions (e.g., Na^+ or K^+) (Duxson et al., 2006; Buchwald et al., 2011). Recent research has indicated that the hydroxyl free radicals ($\cdot OH$) released in the alkaline solutions catalyze the disintegration of the aluminosilicate precursor by breaking the bonds of Si-O-Si, Al-O-Si, and Al-O-Al, besides catalyzing the promotion of isolated aluminate and silicate anions reconstruction via remaking the bonds of Si-O-Si, Al-O-Si, and Al-O-Al (Feng et al., 2016). Thus, the tetrahedrons of silicon and aluminum are combined by oxygen bridges to form the high-connectivity chain or ring network structures. The negative charge given by tetra-coordinated aluminum is compensated by the alkali metal ions (Xu et al., 2001). However, the lower-silica gels in such geopolymer matrix (e.g., high molar ratio of Na_2O/SiO_2 in the activating solution or low molar ratio of Si/Al in the aluminosilicate source) tend to be transformed into some loose particulate units [i.e., pseudo-zeolitic structure (mainly Q^4)] rather than continuous well-connected N-A-S-H gels (He et al., 2013; Provis et al., 2015). It was found that a reasonable content of silicate species in the activating solution could yield compact alkali-aluminosilicate geopolymer matrix with more continuous gels, especially when using the solid aluminosilicate precursor with lower Si/Al ratio (Duxson and Provis, 2008).

The results of solid-state nuclear magnetic resonance (NMR) confirmed the chemical environment of silicon and aluminum in the calcium-free geopolymer made by low-impurity aluminosilicate precursor (Buchwald et al., 2007). The
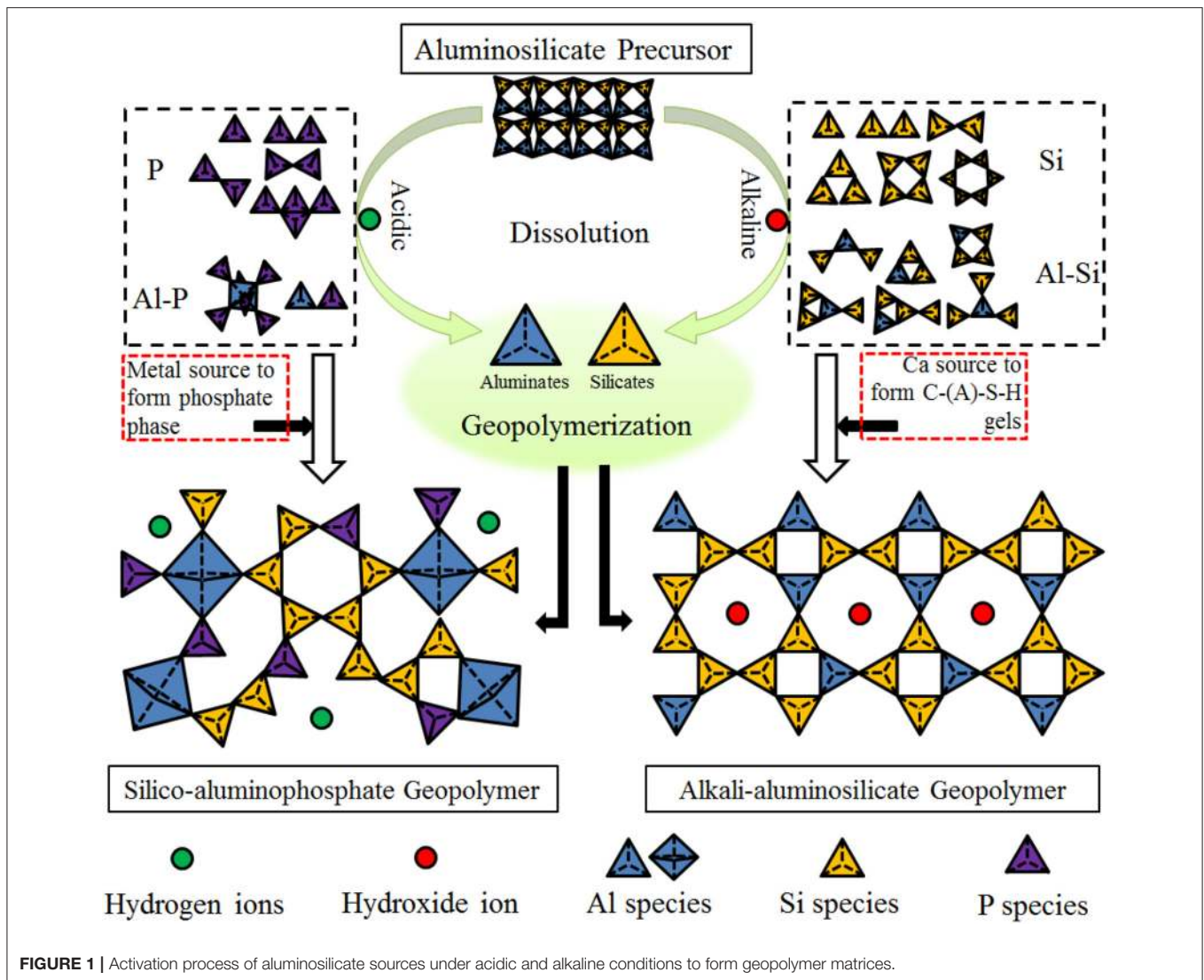
FIGURE 1 | Activation process of aluminosilicate sources under acidic and alkaline conditions to form geopolymer matrices.

higher intensity of the Q^4(4Al) and AlO$_4$ signals shown by NMR curves indicated that the tetra-coordinated silicate and aluminate species dominate the N-A-S-H gels formed in alkali-aluminosilicate geopolymer (Xu et al., 2018).

The microstructure and strength developments of the low-calcium FA-based geopolymer activated by an alkaline solution were descriptively explained beforehand (Fernández-Jiménez et al., 2005, 2006). When reacted with alkaline solution, the FA grains are chemically opened which dissolves the active silicate and aluminate phases to form microscopic imperfections (e.g., points or holes). The dissolved species are condensed into gels through geopolymerization and nucleation which result in compact geopolymer matrix with relatively adequate strength (Pacheco-Torgal et al., 2008). A three-stage corresponding relationship between microstructure evolution and geopolymerization is established to interpret the mechanical strength development in the AAS geopolymer (Fernández-Jiménez et al., 2006). The first stage is the "dissolution stage" of the glassy aluminosilicate phases. Since the matrix is not

yet formed during this period, no mechanical strength can be achieved. The second stage is the "induction period," where massive metastable gels (denoted Gel 1 in Fernández-Jiménez et al. (2006)) are formed and precipitated. As the dissolution of silicate is comparatively slower than that of aluminate, the Gel 1 includes relatively high amount of reactive aluminum which is associated with the initial setting of the geopolymer paste. It is good to mention that the mechanical strength development is usually initialized at the second stage. The final stage is the "silicon incorporation stage" that describes the transformation of Gel 1 into Gel 2 (as indicated in Fernández-Jiménez et al., 2006) wherein the reactive aluminum is embedded into the Si-rich gels to form Gel 2. According to the aluminosilicate precursor and activator used, the mechanical strength of the formed matrix will usually be lower when the content of Gel 1 is higher than that of Gel 2 in hardened geopolymer matrix. Conversely, the mechanical strength can be higher in case the content of Gel 2 outnumbers that of Gel 1, as reported by Criado et al. (2008).
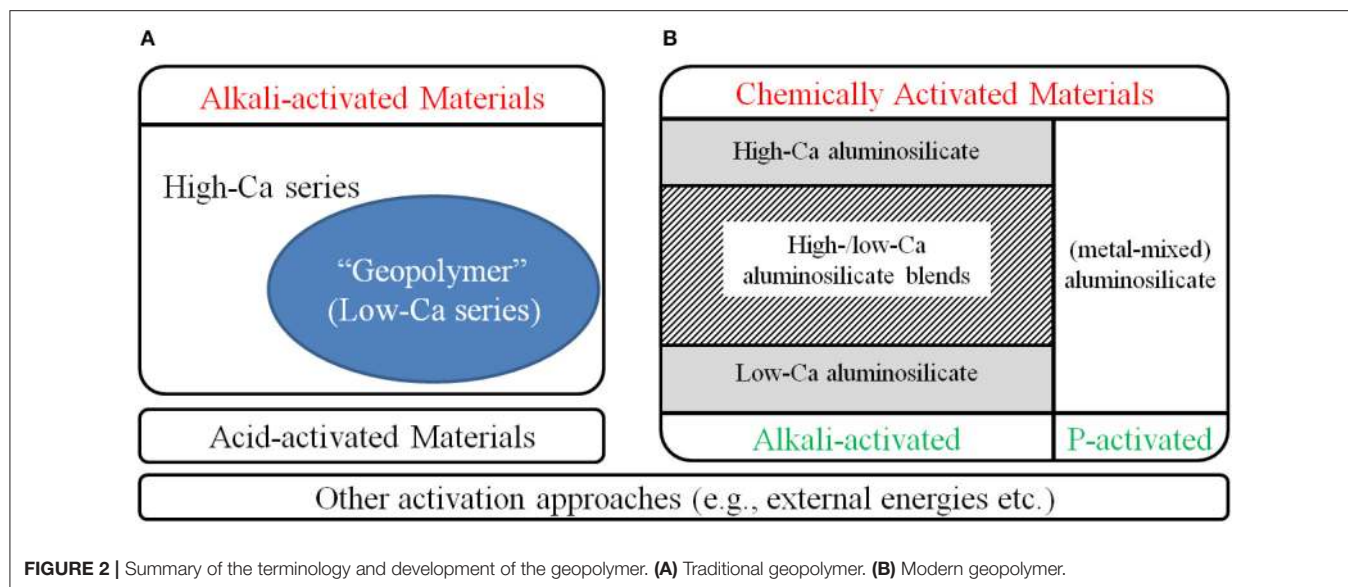
FIGURE 2 | Summary of the terminology and development of the geopolymer. **(A)** Traditional geopolymer. **(B)** Modern geopolymer.

Effect of "Impurities" in AAS Geopolymer

Regarding the role of calcium in alkali-aluminosilicate geopolymer, it is usually claimed that calcium aluminate silicate hydrate (C-A-S-H) gels with tobermorite-like structure (mostly Q^2 and some Q^1) are generated during the geopolymerization (Richardson et al., 1994). The calcium source can induce the aluminosilicate precursor to produce different chemical products in AAS geopolymer. The chemical environments of silicon in calcium-incorporated AAS geopolymer behave as Q^1 and $Q^2(1Al)$ forms, while the $Q^4(2Al)$, $Q^4(3Al)$, and $Q^4(4Al)$ chemical forms of silicon appear in calcium-free AAS geopolymer (Buchwald et al., 2007). The AlO_4-dominated C-(A)-S-H gels and the hydrotalcite (AlO_6) exist in the calcium-incorporated AAS geopolymer as the main chemical configurations of aluminum, which shows significant differences compared to calcium-free AAS geopolymer (AlO_4-dominated N-S-A-H gels).

The combined utilization of GGBS and low-calcium FA can produce N-A-S-H and C-A-S-H gels which are entangled together to form strength-giving gels. The molecular structure of C-A-S-H gels in high-calcium AAS geopolymer can be generalized as the Al-substituted C-S-H gels (Richardson et al., 1993; Brough et al., 2001; Lodeiro et al., 2010). Such gels have Ca/Si ratio lower than that formed in Portland cement (Wang and Scrivener, 1995). This interpretation is similar to the chemistry of supplementary cementitious materials (SCMs) in OPC. The Si-rich phase improves the lower Ca/Si ratio of hydrates by consuming portlandite (i.e., pozzolanic reaction), while Al-rich phase promotes the Al-uptake of hydration products (Lothenbach et al., 2011).

Although the glassy aluminosilicate source with high calcium content can easily generate C-A-S-H gels in alkali environment, the reactivity of available calcium in raw materials may be varied substantially depending on its existence forms. Besides, the GGBS and high-calcium FA have similar calcium and glassy aluminosilicate contents, yet they behave differently in the alkali activation process. The high reactivity of GGBS is mainly attributed to the fast cooling technology (e.g., water quenching granulation) which generates amorphous phases with the network-forming anions $[SiO_4]^{4-}$, $[AlO_4]^{5-}$, and $[MgO_4]^{6-}$ in addition to the network-modifying cations Ca^{2+}, Al^{3+}, and Mg^{2+} (Garcia-Lodeiro et al., 2015). The existence of calcium species can lower the polymerization degree of silicon network which can equip the GGBS with high pozzolanic activity. On contrary, the high-calcium FA particles usually form crystalline phases (e.g., mullite and quartz) due to the slow cooling collection method which presents minimal or no cementitious properties. Therefore, the use of high-calcium FA as main raw material for the preparation of alkali-aluminosilicate geopolymer is significantly challenging at room temperature.

In many existing studies on the durability and mechanical properties of AAS geopolymers regardless of "two-part" (i.e., liquid activators) or "one-part" (i.e., solid activators) mixing approaches, the use of GGBS and FA combination with a certain ratio as an aluminosilicate precursor achieves a geopolymer binder that can roughly meet the engineering requirements (Ismail et al., 2014; Bernal et al., 2015, 2016; Alrefaei and Dai, 2018; Alrefaei et al., 2019). The incorporation of high-calcium materials (i.e., to seed calcium species) with low-calcium raw materials (i.e., main source of alumina and silica) greatly affects the formation of the main binding gels (Bernal et al., 2016). The N-A-S-H type gels generated in low-calcium systems exhibit a relatively slower reaction rate compared to the C-A-S-H type gels in high-calcium systems; however, N-A-S-H gels promote highly cross-linked and compact products through extending the curing time (Bernal et al., 2016). In other words, the synergistic effect of the high- and low-calcium aluminosilicate precursors is witnessed in the coexistence of these molecular structures, where the C-A-S-H gels ensure early performances (e.g., setting time and early strength), while the N-A-S-H

gels contribute to long-term characteristics (e.g., durability and strength development).

SAP Geopolymer

The Egyptian pyramids proved their reliability and durability for thousands of years although the construction materials used in the Pyramids are not fully clear (MacKenzie et al., 2011). However, limited research declared that the surface of pyramids' blocks spontaneously grew a white/red coating that was complicated geopolymeric phosphate compounds made of crystalline hydroxyapatite and brushite embedded in a poly(sialate)/SiO$_2$ matrix (Barsoum et al., 2006; Davidovits, 2011). Later on, the aluminosilicate precursors consolidated by phosphates or orthophosphoric acids were explored for preparing refractory castables (Kingery, 1950, 1952) which can be defined as phosphate activation of the aluminosilicates to yield an SAP geopolymer with excellent durability and high temperature resistance (Wagh, 2016). The use of phosphate or phosphoric acid as an activator allows the chemical interaction with the aluminosilicates to produce geopolymeric binder with condensed poly(silico-alumino-phosphate) phases (Cao et al., 2005; Liu et al., 2010).

Regarding the molecular structure in SAP geopolymer, the $[AlO_4]^{5-}$, $[SiO_4]^{4-}$, and $[PO_4]^{3-}$ units act as basic blocks (He et al., 2013). Compared with AAS geopolymer, the $[PO_4]^{3-}$ unit replaces the alkali metal ion, as reported by Cui et al. (2011). Cui's model revealed that partial replacement of $[SiO_4]^{4-}$ unit by $[PO_4]^{3-}$ in the broken Si-O-Al bonds may occur in low polymeric network. Thus, the charge balance within the molecular structure can be achieved without the involvement of monovalent cations. Previous research showed that the updated Si-O-Al linkage (i.e., Al-O-P) can balance the charge due to the aluminum chemical shift ranging from octahedral or/and pentahedral coordination to tetradentate form (Cao et al., 2005). However, many studies indicated that the hexa-coordinated aluminum dominates in SAP geopolymers (Davidovits, 2011; Louati et al., 2014, 2016). It should be noted that an amorphous Si-Al-P structure was reported in AAS geopolymer wherein the tetrahedral P was identified to occupy a proportion of site of silicate (Mackenzie et al., 2005).

Since the model of microstructure evolution of SAP geopolymer was barely reported in previous literature, some result-derived interpretations and hypotheses are introduced in this paper based on existing studies (Duxson et al., 2006; Cui et al., 2008, 2011; Wagh, 2016). Cui et al. (2011) synthesized SAP geopolymer using pure Al$_2$O$_3$-2SiO$_2$ powders (synthesized in the lab) and phosphoric acid with P/Si molar ratio of 1.2. The XRD patterns showed no clear trace of newly-formed crystalline peaks in the phosphate activated geopolymers. Instead, a broad diffused peak in the range of 15–40° (2θ) appeared in all the samples. The diffraction peak was shifted from 22° (2θ) in calcined Al$_2$O$_3$-2SiO$_2$ powder to about 26° (2-theta) in geopolymers, with a marginal change in the diffraction intensity. It was claimed that the molecular structure and interlayer spacing were chemically shifted after geopolymerization in acid phosphorus environment relative to the raw Al$_2$O$_3$-2SiO$_2$ powders.

Besides, the natural aluminosilicate materials like Tunisian clay and metakaolin were also investigated when activated by phosphate acid with various Si/P molar ratios (Douiri et al., 2014; Louati et al., 2014). A shift in the wide broad band from 18–30° (2θ) to 22–35° (2θ) was observed in both calcined clay and synthesized geopolymers, as well as the diffraction intensity changed in some crystalline peaks e.g., aluminum phosphate (AlPO$_4$), augelite (Al$_2$(PO$_4$)(OH)$_3$), and monetite (CaHPO$_4$). Such differences in the XRD patterns of the raw aluminosilicates and phosphate activated aluminosilicates (i.e., SAP geopolymer) could be attributed to the geopolymerization of the aluminosilicate precursors.

Perera et al. (2008) also performed a comparative study on the metakaolin-based geopolymer when activated by alkali and phosphate solutions. Similar to Cui et al. (2011) observations, the XRD results confirmed the amorphousness of SAP geopolymer. Further investigations by the transmission electron microscope (TEM) equipped with energy dispersive X-ray spectroscopy (EDXS) and selected area electron diffraction (SAED) indicated that such amorphous phases contained Si, Al, P, and O. The SAED image exhibited some blurred rings and spots instead of crystal lattices which further ensured the availability of amorphous phases in SAP geopolymer (Perera et al., 2008).

Furthermore, magic angle spinning-nuclear magnetic resonance (MAS-NMR) analysis was conducted on the SAP geopolymer by Perera et al. (2008). A single $[PO_4]^{3-}$ resonance was observed at around −16 ppm which could be deconvolved into two resonances (−4 and −16 ppm) due to its asymmetric line shape. A cross polarization (CP) NMR of P was identified to enhance the dominance at −16 ppm. The ^{27}Al results indicated that the main chemical environment of aluminum in SAP geopolymer was six-coordination (VI) as evidenced by the single resonance at an apparent shift of around −12 ppm. Thus, the phosphate activation promoted the metakaolin to produce mixed octahedral Al(VI) environment with both P and Si, which influenced the oxo-bridged second coordination sphere. This was mainly unlike the AAS geopolymer where Al(VI) was converted to tetrahedral sites, i.e., Al(IV). The three resonances (e.g., −91.8, −101.6, and −110.8 ppm) in ^{29}Si NMR curve described the Q^3, Q^4 (Al or P), and Q^4 silicon chemical environments, respectively (Provis et al., 2015). The intensity of Q^3 was the lowest which meant that most of metakaolin was dissolved. The mixed environment of Si-Al-P phase in SAP geopolymer was assigned as the Q^4 (Al or P), while the Q^4 was described as siliceous or Al-free portions that might not fully connect to P phase (Cao et al., 2005).
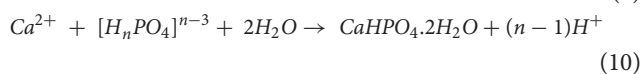
Effect of "Impurities" in SAP Geopolymer

In order to improve the modest early performance of SAP geopolymer, the incorporation of some alkali metals as setting agents (e.g., solid Mg/Ca source) with aluminosilicate precursors can produce a setting-controlled SAP geopolymer matrix (Luz et al., 2015). Such agents essentially initiate acid-base chemistries (i.e., between phosphate and setting agents) in addition to geopolymerization of the aluminosilicates, which enables the fast formation of amorphous or crystalline phosphates to modify the workability and early strength of such geopolymer (Wang

et al., 2018b). Relative to the aluminosilicate precursors, the added setting agents can be regarded as "impurities" here. The chemistry of such setting agents is elaborated below.

"Phosphate cement" is a general term that describes the phosphate as a main ingredient of the cement (Walling and Provis, 2016). Since phosphate cement is usually a binder that hardens through acid-base and/or hydrolysis chemical reactions (usually generate crystalline phosphates as main products) at room temperature, it is also named as chemically bonded phosphate ceramic (CBPC) (Roy, 1987). CBPCs were discovered and developed as dental cements in the nineteenth century which were extended to construction field later on as patching materials for rapid rehabilitation of runway and bridge. The formation of CBPC experiences the dissolution of alkali metals and phosphates to form crystalline structures (i.e., phosphate compounds) with excellent adhesive and mechanical properties. It is expected that such chemical mechanism (i.e., the chemistry between alkali metals and phosphates) can be introduced into SAP geopolymer as a room temperature hardening mechanism to address its weak early properties (Wang, 2018). The reaction products of CBPCs are directly linked to the raw materials used; more specifically, the material recipe (e.g., ratio, reactivity etc.) is related to the reaction environments (e.g., pH condition, ions concentration etc.). Here, the calcium- and magnesium-based sources are comprehensively introduced because other alkali-metal sources (e.g., Fe and Zn) fails to form well-crystallized phases due to the violent reaction process (Wagh and Jeong, 2003a,b).

Calcium-based CBPC is often termed as "calcium phosphate cement" (CPC) which is used as a bioceramic material in orthopedic industry due to its excellent bioactivity and biocompatibility (Ben-Nissan, 2014). The chemical reactions involved during the CPC setting consist of three stages: dissolution, supersaturation, and precipitation (Zhang J. et al., 2014). In acidic phosphate solution, the calcium donors slowly release the calcium ions and react with (hydro)-phosphate groups to form a supersaturated solution (i.e., paste). When reaching the critical values (e.g., ions concentration or pH condition), the nucleated and precipitated new phase grows along with the continuous dissolution of calcium. According to the composition of final products, the CPC is classified into apatite cement [β-tricalcium phosphate, $Ca_5(PO_4)_3(OH/Cl/F)$ or $Ca_3(PO_4)_2$] and brushite cement ($CaHPO_4·2H_2O$) (Tamimi et al., 2012; Ben-Nissan, 2014). In general, according to the recipe (e.g., solubility and Ca/P ratio) and reaction conditions (e.g., pH value and hydrothermal environment), the possible chemical processes involved in the formation of CPC matrix can be described in Equations (8–10).

$$3Ca^{2+} + 2[H_nPO_4]^{n-3} \rightarrow Ca_3(PO_4)_2 + 2nH^+ \quad (8)$$

$$5Ca^{2+} + 3[H_nPO_4]^{n-3} + H_2O \rightarrow Ca_5(PO_4)_3(OH) + (3n+1)H^+ \quad (9)$$

$$Ca^{2+} + [H_nPO_4]^{n-3} + 2H_2O \rightarrow CaHPO_4.2H_2O + (n-1)H^+ \quad (10)$$
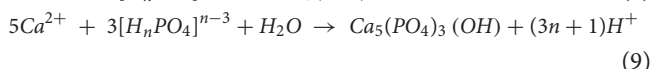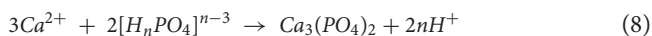
Fresh CPC is a castable paste which is preferable for bone defects reconstruction with minimum invasive surgery since it can be resorbed under physiological conditions after embedding into the body (Xue et al., 2012; Inzana et al., 2014; Xu et al., 2017). Thus,

the moldable properties of calcium-blended SAP geopolymer extend its applications to 3D printing for building arts in civil engineering or other aesthetic fields.

Magnesium phosphate cement (MPC) is another typical CBPC that is widely used in civil engineering because of its excellent performance (Wang and Dai, 2017). In the early research stage, the MPC was fabricated with magnesia and phosphoric acid (Wagh, 2016). The lower pH environment induces a rapid and highly exothermic reaction where the reaction product is water-soluble magnesium dihydrogen phosphate [$Mg(H_2PO_4)_2·nH_2O$]. Subsequently, attempts were made to use less acidic diphosphate. The employment of diphosphate and calcined magnesia further mitigates the reaction rate and heat release during MPC formation. The soluble diphosphates can create an acidic environment in water which facilitates the dissolution of magnesia. When the concentration and pH are approaching ideal value, crystal generation and growth occur in the supersaturated slurry (Chauhan et al., 2008). The general reaction of MPC is described in Equation (11). The resulting phase is crystalline struvite or its analogs (e.g., struvite-K or struvite-Na) with 6–8 crystal waters (Chauhan et al., 2011; Chauhan and Joshi, 2014). Such hydrates have excellent cementitious and mechanical properties (Ding et al., 2012). Finch and Sharp (1989) also studied the reaction of mono-aluminum phosphate and magnesia in terms of molar ratio and final products, showing that the crystalline Newberyite ($MgHPO_4·3H_2O$) appeared instead of struvite analog in case of the Mg/P molar ratio of 4. The phosphate species might involve in the formation of amorphous phase as well.

$$MgO + XH_2PO_4 + nH_2O \rightarrow MgXPO_4 \cdot (n+1)H_2O \quad (11)$$
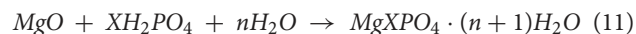
The characteristics of crystalline calcium/magnesium phosphate phases including mineral name, chemical formula and main application fields are listed in **Table 1**. Ca-based apatites are mostly used as biomaterials for dental applications and mimic bones due to their good biocompatibility (Xu and Simon, 2005; Giocondi et al., 2010). The variants of Ca-based apatites can also be employed to immobilize the heavy metal pollutants (e.g., Pb, Cd, Zn, or Cr) by embedding them into the respective apatite minerals (e.g., Ca/Zn replacement) (Saxena and D'Souza, 2006). On the other hand, the final products containing struvite or its analogs (i.e., Mg series) are usually used as rapid repair materials in civil engineering due to their high mechanical performance and adhesive property (Ma et al., 2014).

Model Comparison of AAS and SAP Geopolymers

Alkali activation process of Ca sources (i.e., C-A-S-H gel formation) and acid-base reaction process of Ca/Mg and phosphate (i.e., amorphous or crystalline phosphates) can promote both rapid setting at room temperature and strength upscaling by forming new phases. Their simplified synthesis models of the two "Hybrid" geopolymers are conceptualized in **Figure 3**.

Figure 4 shows a comparative flow chart between the formation processes of AAS and SAP geopolymers wherein

TABLE 1 | Specific crystalline products in calcium/magnesium phosphate cement.

Mineral name		Chemical formula	Application
Ca series	Brushite/Monetite	$CaHPO_4 \cdot 2H_2O/CaHPO_4$	
	Hydroxyapatite (HAp)	$Ca_5(PO_4)_3 \cdot OH$	Biomaterial, Phosphor
	Chloroapatite (ClAp)	$Ca_5(PO_4)_3 \cdot Cl$	material,
	Fluoroapatite (FAp)	$Ca_5(PO_4)_3 \cdot F$	Waste treatment
Mg series	Struvite	$Mg(NH_4)PO_4 \cdot 6H_2O$	
	Struvite-K (Ceramicrete)	$MgKPO_4 \cdot 6H_2O$	Building material,
	Struvite-Na	$MgNaPO_4 \cdot 7H_2O$	Waste encapsulation
	Newberyite	$MgHPO_4 \cdot 3H_2O$	

FIGURE 3 | Simplified conceptual models of two "Hybrid" geopolymers. **(A)** Hybrid AAS Geopolymers. **(B)** Hybrid SAP Geopolymers.
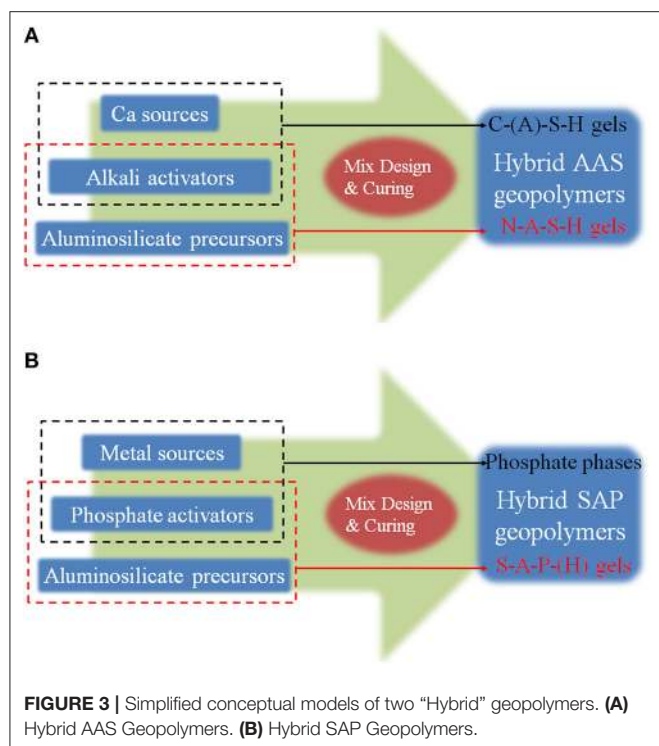
the key stages from the raw materials to the final geopolymer binders are outlined. The Ca-containing AAS geopolymer was investigated for many years (as shown in **Figure 4A**), including dissolution, speciation, gelation, reorganization and final polymerization (Duxson et al., 2006). The chemically-dissolved aluminosilicate precursors accessibly form the C-(A)-S-H gels when encountering the free Ca species. This chemical process is relatively faster than that of N-A-S-H gels at ambient temperature. In most cases, the two gels co-exist in the final geopolymer matrix as resulting products.

As a comparison, the synthesis process of SAP geopolymer is simplified in **Figure 4B**. However, the research related to SAP geopolymer is rare, so it should be noted that the synthesis process of such geopolymer is deduced according to the classical interpretations on the CBPC and the AAS geopolymer. The transformation of phosphate species from sol state to gel state, including the dissolution and speciation of (hydro)-phosphate ions, is the first step during SAP geopolymer formation (Perera

et al., 2008). Usually, the acid-base reaction between Ca or Mg sources and (hydro)-phosphate ions is initiated before the dissolution of aluminosilicate precursors. The gelation and reorganization among aluminate, silicate and phosphate form S-A-P gels via the condensation processes. Final polymerization of these species gradually synthesizes the SAP geopolymer matrix. Unlike AAS geopolymer, phosphate-bearing crystalline or amorphous phases may occur in some cases when reasonable molar ratios (metal ion to phosphorus) and pH environment are available (Guo et al., 2016).
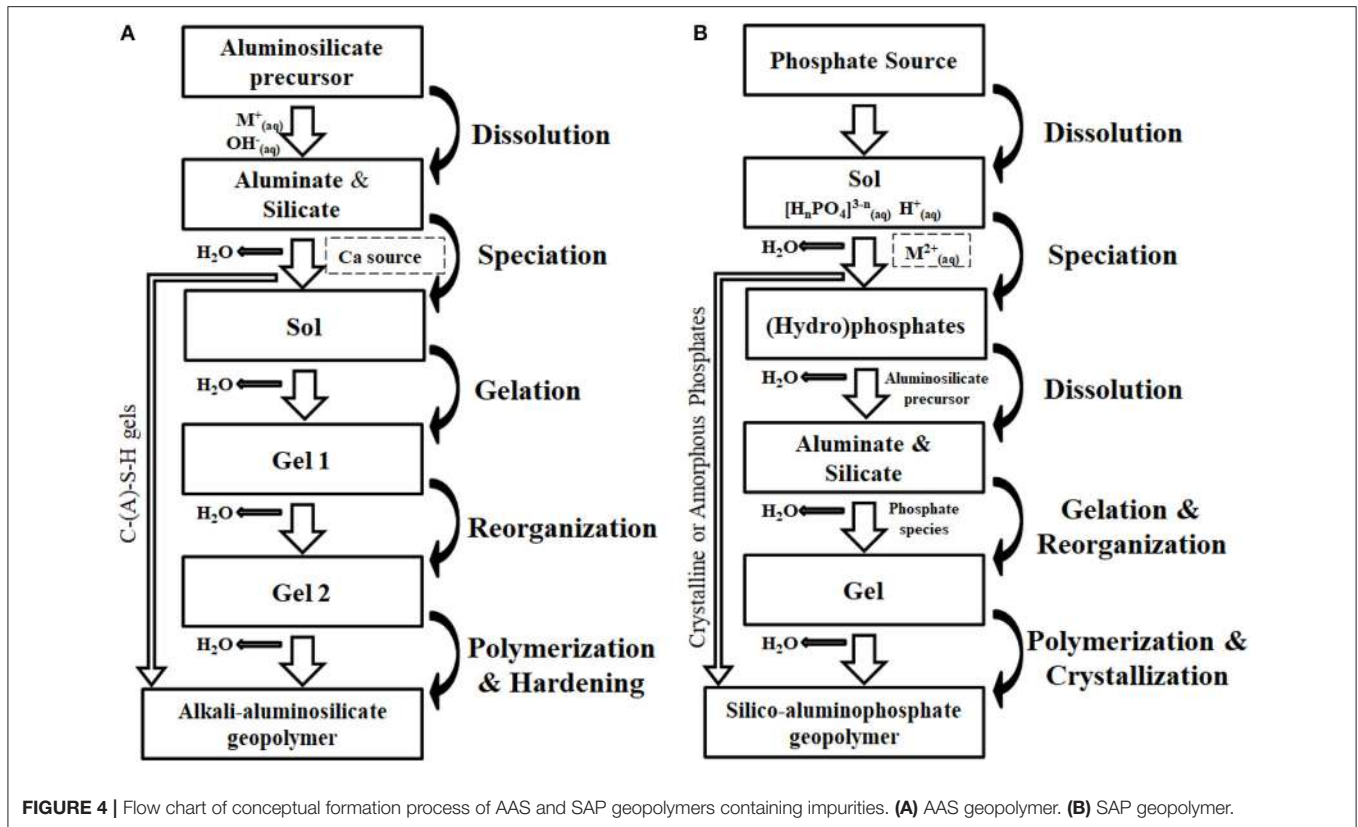
ENVIRONMENTAL IMPACT

Portland Cement and Geopolymer Binders

Due to the vast of mineral resource consumptions, intensive energy usage and high carbon emissions companioned with ordinary Portland cement (OPC) production, it is believed that the geopolymer binders should be strongly proposed as green building materials to partially replace cement in future construction applications (Walkley et al., 2017). Usually, the life cycle assessment (LCA) methodology, also known as the "cradle to grave" approach, is internationally normalized to provide quantitative information for the environmental burden of each product manufacture system (ISO, 2006; Passuello et al., 2017). However, the recent findings related to the LCA-based comparison between geopolymer and OPC products showed a wide variation, even some conflicting results, depending on the goal, scope, the needs, and the targeted audience used in LCA analysis (Ouellet-Plamondon and Habert, 2015).

The aroused controversies regarding the LCA of geopolymer binders are derived from several complexities such as the local resources availability, the process of raw materials, thermal treatment and the mix design parameters (e.g., alkali content, Si/Al molar ratio, water-to-binder ratio etc.), as shown in **Figure 5** (Duxson et al., 2007; Habert et al., 2011; Ouellet-Plamondon and Habert, 2015; Habert and Ouellet-Plamondon, 2016). Another challenge of the LCA application in geopolymer binders is that such binders mainly include two different industrial products (i.e., aluminosilicate precursors and activators) unlike the OPC that deals with a single material industry. When the solid precursor is treated as a waste material in the LCA analysis (e.g., in Europe, *Directive 2008/98/EC of the European Parliament and of the Council on waste and repealing certain Directives*. L312: 3–30), the energy consumed during the production process (i.e., FA and GGBS from power stations and steel production, respectively, as shown in **Figure 5**) does not negatively impact the CO_2 balance of the geopolymer binders. As a comparison, the cement clinker calcination consumes a large quantity of fossil fuel energy and releases additional CO_2 through the decarbonation reaction. Thus, the geopolymer binders are considered as a groundbreaking solution for the environmental issues caused by Portland cement industry (Duxson et al., 2007). On the other hand, such binders adversely impact the environment when the precursor is considered as a raw material since the thermal input of the solid precursor should be involved in the LCA calculation. Besides, Habert et al. (2011) claimed that the production of a typical AAS

FIGURE 4 | Flow chart of conceptual formation process of AAS and SAP geopolymers containing impurities. **(A)** AAS geopolymer. **(B)** SAP geopolymer.

geopolymer concrete presents a slightly lower impact on the global warming compared to standard OPC concrete, mainly due to the energy expenditure of activators (e.g., mining, treatment, manufacture, and transport). Regarding the SAP geopolymer, it was reported that the energy usage during the production of phosphate binders (mainly the phosphate products) accounts for around one-fourth of that consumed in Portland cement industry (Wagh, 2016).

AAS and SAP Geopolymers

When comparing the two types of geopolymer (i.e., AAS and SAP), the key point lies in the environmental impact of activating solutions. During the preparation of AAS geopolymer, it is necessary to use soluble sodium silicates to address the performance requirements (e.g., mechanical properties; Ding et al., 2016) of geopolymer concrete, especially when aluminosilicate precursors with lower Si/Al ratio is employed (Krizan and Zivanovic, 2002). However, the silicate solutions are always contentious due to their high cost and aggressiveness to the environment during production (e.g., intensive energy consumption and global warming potential) (Fawer et al., 1999). On the other hand, for SAP geopolymer, the phosphate solutions are majorly manufactured through the reaction between phosphate rock and sulfuric acid at <100°C. Thus, the environmental impacts of the phosphate solutions are largely determined by the sulfuric acid production industry (Kongshaug, 1998). Generally, modest emissions (e.g., carbon dioxide) are linked to the modern sulfuric acid production

industry. Besides, the exothermic reactions involved in such production may generate net energy (i.e., heat released) that can be totally employed in other industries (Wood and Cowie, 2004). Further, emission standard of pollutants for sulfuric acid industry is severely implemented all over the world (*China Emission Standard of Pollutants for Sulfuric Acid Industry*, 2011; *EU Best Available Techniques for Pollution Prevention and Control in the European Sulphuric Acid and Fertilizer Industries*, 2000; *US Guidelines for Limitation of Contact Sulfuric Acid Plant Emissions*, 1971). Accordingly, the phosphate solutions seem to be more sustainable and environmentally friendly relative to the alkali-silicate solutions in terms of the gas emission and energy expenditure.

In addition to their moderate carbon emissions and energy consumption, the application of the SAP geopolymer products may form a virtuous eco-system as the phosphorus available in such binders can be absorbed or extracted to form the P-containing fertilizers for crops after abandoning (Bartos et al., 1991; Raven and Loeppert, 1996). These biological and chemical actions may further form mineral deposits (e.g., phosphate rocks). Such eco-friendly loop makes the phosphate-based products greener and more sustainable which meets the concept of industrial ecology in the long run (Jelinski et al., 1992). Adversely, the alkali-silicate activators (varying modulus of sodium silicate) used for preparing the AAS geopolymer products are usually non-recyclable. Some researchers are exploring some waste-derived activators (e.g., silica fume and rice husk ash) and non-silicate activators (e.g., carbonate and sulfate)
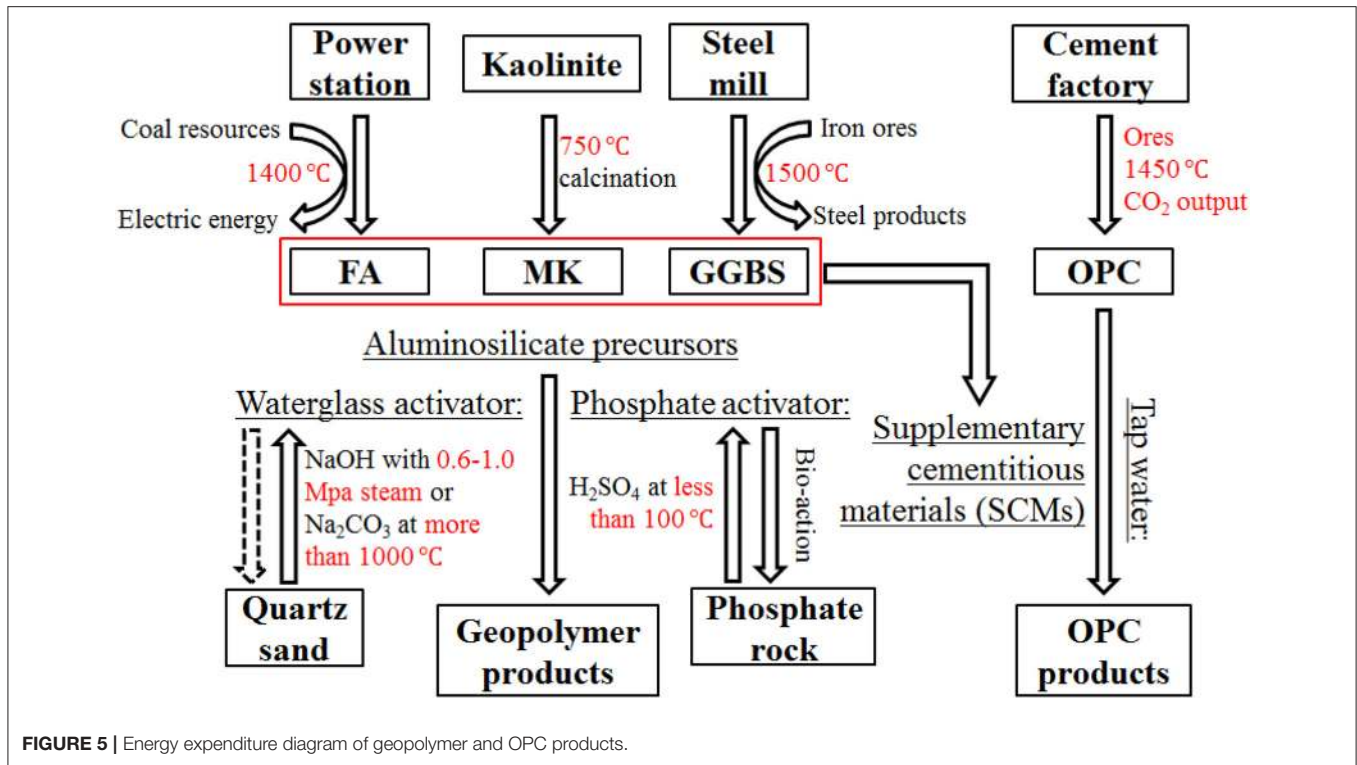
FIGURE 5 | Energy expenditure diagram of geopolymer and OPC products.

to replace commercial silicate solutions for AAS geopolymer preparation (Nazari et al., 2011; Bernal et al., 2012; He et al., 2013), which may reduce environmental burden caused by waterglass industry.

PERFORMANCE, DURABILITY, COST, AND ACCESSIBILITY

Compressive Strength

The mechanical strengths reported in the published literature varied widely owing to the differences in raw materials (e.g., attribute and recipe), curing condition (e.g., temperature and moisture) and sample preparation technology (e.g., size and age). The 28 days compressive strengths of the geopolymer obtained from literature survey, including low- and high-calcium AAS geopolymers in addition to SAP geopolymers, are shown in **Figure 6** (Davidovits, 2011; Chindaprasirt et al., 2012, 2013b; Nath and Kumar, 2013; Nematollahi and Sanjayan, 2014; Atiş et al., 2015; Guo et al., 2016; He et al., 2016; Reddy et al., 2016; Wang et al., 2016; Wang, 2018). Clearly, the statistics showed that the compressive strengths of the AAS geopolymer (i.e., 15–65 MPa for low-calcium series and 70–110 MPa for high-calcium series) significantly outperformed that of the SAP geopolymer (i.e., 10–50 MPa).

Ding et al. (2016) summarized the mechanical properties of AAS geopolymer concrete, revealing that the compressive strength and elastic modulus can moderately meet the requirements of Portland cement concrete design codes. Reddy et al. (2016) made an attempt to investigate the influences
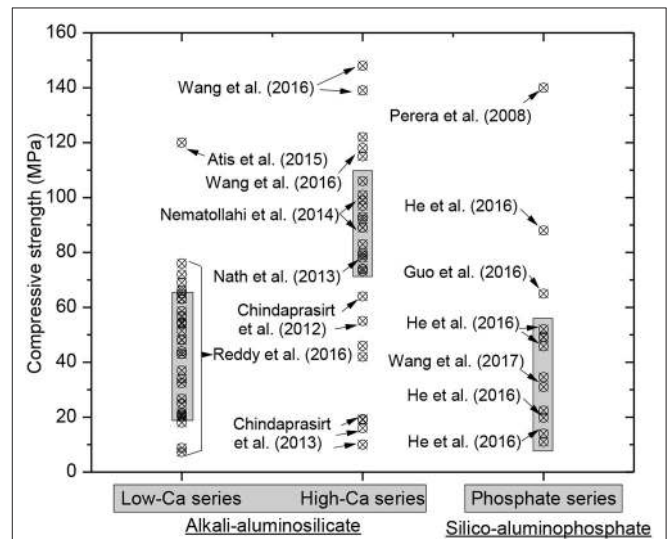

FIGURE 6 | Literature survey on 28 days compressive strength of the geopolymer binders. It should be noted that the statistics ignore the attribute and recipe of raw materials and curing conditions used.

of oxide composition of precursors on the compressive strength of the AAS geopolymer products. Perera et al. (2008) synthesized (60°C curing for 24 h) SAP geopolymer with compressive strength approaching 140 MPa which is two-fold that of AAS geopolymer. On the other hand, Wang et al. (2017) reported that the final setting time was more than

48 h and the compressive strength reached 31 MPa at 28 days for the metakaolin (MK)-based geopolymer activated by mono-aluminum phosphate at room temperature curing. Guo et al. (2016) obtained the phosphate-based geopolymer using MK and disused phosphate liquid which resulted in a compressive strength of 62–67 MPa when the matrix experienced 7 days curing at 60°C. The activating effect of disused phosphate liquid exceeded that of phosphoric acid because of the presence of aluminum ions and thermal curing.

Thermal Stability, Dielectricity, and Efflorescence

As previously reported, the MK-based geopolymers activated by phosphoric acid exhibited good thermal and volume stability (Liu et al., 2012). Phase transition (from aluminum hydrogen phosphate to berlinite) was observed when the geopolymer sample was subjected to elevated temperatures (900–1,550°C). In the AAS geopolymer, the presence of calcium source could reduce the curing cost and increase early strength as previously explained. The early compressive strength of such hybrid geopolymer matrix is augmented along with the increased use of GGBS (Guerrieri and Sanjayan, 2010). However, such practice lowers the ability of geopolymer to resist fire and high temperatures (Buchwald et al., 2007) due to the existence of the non-fire-resistant C-(A)-S-H gels.

Cui et al. (2011) compared the dielectric loss of two types of geopolymers. It was found that the SAP geopolymer held a very low dielectric loss (around 0.01 for frequencies more than 300 MHz) at 300°C dried for 2 h. On the other hand, the AAS geopolymer was temperature-dependent due to the availability of free metal and hydroxyl ions; thus, it was difficult to decrease the dielectric losses resulting from ion transfer.

Besides, the efflorescence is also a serious issue with relatively little attention in research (Najafi Kani et al., 2012; Allahverdi et al., 2015; Pacheco-Torgal, 2015). Efflorescence in AAS geopolymer is the result of the incomplete consumption of alkaline and/or soluble silicates that leads to form sodium carbonate in the pores or on the surface of geopolymer matrix (Xue et al., 2018). This can be because the presence of water weakens the bond of sodium in geopolymer; besides, the efflorescence rate is strongly activation-dependent. In case of the same alkali content and curing temperature, NaOH-activated geopolymers show less and slower efflorescence relative to geopolymers activated by sodium silicate. Geopolymers with high Na_2O/Al_2O_3 ratio may suffer from unsightly efflorescence as well (Najafi Kani et al., 2012). The use of calcium blended precursors (i.e., FA/GGBS-based geopolymers) in addition to the hydrothermal curing process usually generates geopolymer binders with relatively weaker efflorescence, yet the GGBS addition appears to delay rather than mitigate the effect of efflorescence (Zhang Z. et al., 2014). Najafi Kani et al. (2012) stated that the alumina-rich admixtures can reduce the efflorescence. Therefore, the well-designed mix proposition and chemical composition of the geopolymer binders can mitigate or even eliminate the efflorescence, e.g., providing hydrothermal curing, sufficient Al-rich mineral admixtures for gel formation and alkali consumption (Allahverdi et al., 2015). On the other hand, SAP geopolymers have high resistance to efflorescence relative to the AAS geopolymers; thanks to the acidic synthesis environment.

Cost and Availability

In addition to the performance comparison, the cost and the availability of both types of geopolymers (i.e., AAS and SAP) are also crucial to practical engineering. Although quotations form regional suppliers (e.g., Alibaba) indicate that the price of phosphoric acid is more than three-fold that of sodium silicate, the SAP geopolymer can act as a complement to AAS geopolymer in the field of geopolymer category. In other words, the SAP geopolymer shall be further explored as small-scale or specifically-required functional materials (e.g., as fire-proof material, dielectric ceramics, coating materials, fast-rapid materials, and 3D printing materials), while the goal of AAS geopolymer is to reduce the traditional cement consumption.

The complexity of aluminosilicate sources, especially aluminosilicate-containing industrial byproducts, is a major concern for geopolymer production. Fly ash as a typical aluminosilicate source for geopolymer preparation is an anthropogenic material with polymorphic, polycrystal, and multi-component system (Blissett and Rowson, 2012). According to different regions, more than 316 individual minerals and 188 mineral groups in coal fly ash have been identified and characterized, which may cause even more differences in non-crystalline phases and particle characteristics (Vassilev and Vassileva, 2005). The diversity of raw materials results in wide differences in the geopolymer mechanical properties, even when using the same formula and mix design. Therefore, if the aluminosilicates are properly characterized, classified and pretreated, the properties of geopolymer products can be tailored for certain applications and performances. The geopolymer turns out to possess multi-phase, multi-component, and multi-morphology; however, its performance is strongly reliable on the types of raw materials. In order to achieve a high performance geopolymer matrix, the following three assessment indices of aluminosilicate are required for preparing different geopolymers (Luxán et al., 1989; De Rojas and Frías, 1996; Agarwal, 2006).

(1) Material characterization: The characterization indices of aluminosilicates include their compositions (oxide and phase) and physical features (particle size, specific gravity, surface, and loss of ignition), which can greatly influence the performances of geopolymer products.

(2) Reactivity test: The reactivity of the aluminosilicate precursors is closely associated with their phases. The combined use of Rietveld analysis (Hill and Howard, 1987) and PONKCS (partial or no known crystal structure; Scarlett and Madsen, 2012) are relatively useful for initial gauging of the crystalline and amorphous phase contents. Glassy phase composition of some aluminosilicates can be captured by SEM-EDXS with multispectral image analysis, to differentiate the inert crystalline and the reactive amorphous phases in case of similar elemental composition (Chancey et al., 2010; Durdzinski

et al., 2015). The participation degree of aluminosilicates during geopolymerization heavily determines the properties of geopolymer products.

(3) Performance enhancements: For improper aluminosilicate sources, particle size reduction and minerals addition seem to be valid. However, the thermal and chemical pretreatments can be more effective because such pretreatments increase the amorphous proportion and decreases the loss of ignition (Handoo et al., 2002; Škvára et al., 2009; Bentz et al., 2012).

POTENTIAL APPLICATIONS

Application in Construction

One of the large-scale applications of geopolymers (mainly AAS geopolymer) is in construction due to their good mechanical behavior and durability. Some modified AAS geopolymer binder has been commercially branded for infrastructure projects, such as PYRAMENT cement (Davidovits, 2011). Currently, the SAP geopolymer is being researched in labs, especially with the focus on the unclear chemistries between phosphate and aluminosilicate. In cases of high-volume content of FA-blended phosphate binder, FA particles are conventionally considered as a diluent or inert filler that modifies the aesthetics of the formed products (e.g., change color and reduce porosity) to be comparable with Portland cement as a rapid healant. Recently, some reports have conversely indicated that the high mechanical strength of the FA-blended phosphate binders is also attributed to the formation of secondary amorphous phase (e.g., phospho-siloxonate geopolymeric phases; Gardner et al., 2015).

Application in Waste Management

The waste production is directly related to population increase. In order to stop the contaminants from flowing into the food chain of human, some effective and low-cost amendments are applied to stabilize/solidify the hazardous or radioactive waste streams (Morrissey and Browne, 2004; Temuujin et al., 2014). According to the definition of stabilization/solidification, stabilization process is defined as the chemical converting of contaminants into their insoluble, immobile or nontoxic forms without spillage, leakage, and disintegration in a long term, while solidification is defined as changing the physical consolidating sludges, liquids, or powders into solid forms so that they will not be dispersed during transportation, long-term storage or disposal. Recently, AAS geopolymer binders are used for the remediation of heavy metals-contaminated soils through stabilization/solidification (S/S) (Luna Galiano et al., 2011). It is claimed that the heavy metals can be fixed in the molecular network during geopolymerization, either chemically through embedment into the molecular structure for charge balance or physically by being trapped in the surrounding 3D network (Van Jaarsveld et al., 1997). In SAP geopolymer, the phosphate ions are also chemically combined with detrimental metal species to form highly insoluble phosphates (e.g., pyromorphite during Pb S/S; Wang et al., 2018a).

Application in Biomaterials

Considering the biocompatibility, resorbability, and customization of living body, the SAP geopolymer with Ca-containing setting agent is considered as an excellent suitable candidate. The tailor-made shape can be pre-prepared using 3D printing technique due to the good injectability of such materials (Chia and Wu, 2015). Except for precast skeletal structure, SAP geopolymer can be injected as a paste into selected regions in the biological body. Not only that paste cements the adjacent tissues, but also has less intrusion properties compared to the implants made of hardened biomaterials. Since bones and teeth mainly contain calcium phosphate compounds, Ca-containing SAP geopolymer can provide the necessary compositions for better biocompatibility. The zinc and magnesium species enable the performance enhancement (e.g., strength) in calcium enriched mixture (CEM) matrix as blended phosphate biomaterials (Utneja et al., 2015). Besides, the viable biocompatible AAS geopolymers have been demonstrated (MacKenzie et al., 2010).

Application in 3D Printing

3D printing is a promising technique that can rapidly manufacture products with spatial complicity and precise distribution (Bassoli et al., 2007; Rengier et al., 2010; Lim et al., 2012). Such attractive rapid prototyping (RP) is based on the additive manufacturing (AM), defined by ASTM International as "the process of joining materials to create objects from 3D model data, usually layer upon layer" (ASTM F2791-10). The customized imaging database (e.g., computed tomography scans) can be visualized via 3D printing system. Nevertheless, how to select the appropriate material with appropriate rheology, setting time, temperature, strength, durability, and other special requirements, is the major problem. Recently, the 3D printing of biomaterials has been applied for surgical planning and prosthetics using phosphate materials due to its biocompatibility in human body (Guvendiren et al., 2016). The "two-part" geopolymer (aluminosilicate and activator) is also potentially applicable for 3D printing in construction (Xia and Sanjayan, 2016; Zhong et al., 2017).

CONCLUDING REMARKS

This paper provides a comprehensive review and comparison between alkali and phosphate activations of aluminosilicate materials. According to the activation mode, the chemically activated aluminosilicates can be termed as alkali-aluminosilicate (AAS) geopolymer or silico-aluminophosphate (SAP) geopolymer, where both of geopolymers need extra promotions (e.g., thermal curing or setting agent) to obtain reasonable engineering properties. The thermal curing is usually inappropriate for *in-situ* applications, while the incorporation of fast-setting chemistries (induced by setting agents) during geopolymerization can easily facilitate an ambient-temperature setting mechanism in geopolymer preparation. Just like the formation of C-(A)-S-H gels in AAS geopolymer, the SAP geopolymer can produce crystalline or amorphous phosphate phases during geopolymerization when metal ions are

incorporated with the aluminosilicates. The different activation modes generate various potential values of these "hybrid" geopolymers in a wide range of research fields. According to the performance, cost and accessibility, the two types of geopolymers are mutually supplemented in terms of function and application fields.

AUTHOR CONTRIBUTIONS

Y-SW collected the data and wrote the paper. YA wrote some parts of the paper besides linguistic and grammar editing. J-GD supervised and finalized the paper.

REFERENCES

Agarwal, S. (2006). Pozzolanic activity of various siliceous materials. *Cement Concrete Res.* 36, 1735–1739. doi: 10.1016/j.cemconres.2004.06.025

Allahverdi, A., Kani, E. N., Hossain, K., and Lachemi, M. (2015). "Methods to control efflorescence in alkali-activated cement-based materials," in *Handbook of Alkali-Activated Cements, Mortars and Concretes*, eds F. Pacheco-Torgal, J. Labrincha, C. Leonelli, A. Palomo, and P. Chindaprasit (Cambridge, UK: Elsevier), 463–483. doi: 10.1533/9781782422884.3.463

Alrefaei, Y., and Dai, J. G. (2018). Tensile behavior and microstructure of hybrid fiber ambient cured one-part engineered geopolymer composites. *Constr. Build. Mater.* 184, 419–431. doi: 10.1016/j.conbuildmat.2018.07.012

Alrefaei, Y., Wang, Y. S., and Dai, J. G. (2019). The effectiveness of different superplasticizers in ambient cured one-part alkali activated pastes. *Cement Concrete Compos.* 97, 166–174. doi: 10.1016/j.cemconcomp.2018.12.027

Arbi, K., Nedeljkovic, M., Zuo, Y. B., and Ye, G. (2016). A review on the durability of alkali-activated fly ash/slag systems: advances, issues, and perspectives. *Ind. Eng. Chem. Res.* 55, 5439–5453. doi: 10.1021/acs.iecr.6b00559

Atiş, C., Görür, E., Karahan, O., Bilim, C., Ilkentapar, S., and Luga, E. (2015). Very high strength (120 MPa) class F fly ash geopolymer mortar activated at different NaOH amount, heat curing temperature and heat curing duration. *Constr. Build. Mater.* 96, 673–678. doi: 10.1016/j.conbuildmat.2015.08.089

Barsoum, M., Ganguly, A., and Hug, G. (2006). Microstructural evidence of reconstituted limestone blocks in the great Pyramids of Egypt. *J. Am. Ceram. Soc.* 89, 3788–3796. doi: 10.1111/j.1551-2916.2006.01308.x

Bartos, J., Mullins, G., Sikora, F., and Copeland, J. (1991). Availability of phosphorus in the water-insoluble fraction of monoammonium phosphate fertilizers. *Soil Sci. Soc. Am. J.* 55, 539–543. doi: 10.2136/sssaj1991.03615995005500020042x

Bassoli, E., Gatto, A., Iuliano, L., and Grazia Violante, M. (2007). 3D printing technique applied to rapid casting. *Rapid Prototyp. J.* 13, 148–155. doi: 10.1108/13552540710750898

Benavent, V., Steins, P., Sobrados, I., Sanz, J., Lambertin, D., Frizon, F., et al. (2016). Impact of aluminum on the structure of geopolymers from the early stages to consolidated material. *Cement Concrete Res.* 90, 27–35. doi: 10.1016/j.cemconres.2016.09.009

Ben-Nissan, B. (2014). *Advances in Calcium Phosphate Biomaterials*. Berlin: Springer. doi: 10.1007/978-3-642-53980-0

Bentz, D. P., Sato, T., De la Varga, I., and Weiss, W. J. (2012). Fine limestone additions to regulate setting in high volume fly ash mixtures. *Cement Concrete Compos.* 34, 11–17. doi: 10.1016/j.cemconcomp.2011.09.004

Bernal, S., Rodríguez, E., Mejía de Gutiérrez, R., and Provis, J. L. (2015). Performance at high temperature of alkali-activated slag pastes produced with silica fume and rice husk ash based activators. *Mater. Constr.* 65, 1–10. doi: 10.3989/mc.2015.03114

Bernal, S. A., Nicolas, R. S., van Deventer, J. S. J., and Provis, J. L. (2016). Alkali-activated slag cements produced with a blended sodium carbonate/sodium silicate activator. *Adv. Cement Res.* 28, 262–273. doi: 10.1680/jadcr.15.00013

Bernal, S. A., Provis, J. L., and Green, D. J. (2014). Durability of alkali-activated materials: progress and perspectives. *J. Am. Ceram. Soc.* 97, 997–1008. doi: 10.1111/jace.12831

Bernal, S. A., Rodríguez, E. D., de Gutiérrez, R. M., Provis, J. L., and Delvasto, S. (2012). Activation of metakaolin/slag blends using alkaline solutions based on chemically modified silica fume and rice husk ash. *Waste Biomass Valoriz.* 3, 99–108. doi: 10.1007/s12649-011-9093-3

Blissett, R. S., and Rowson, N. A. (2012). A review of the multi-component utilisation of coal fly ash. *Fuel.* 97 1–23. doi: 10.1016/j.fuel.2012.03.024

Brough, A., Katz, A., Sun, G.-K., Struble, L., Kirkpatrick, R., and Young, J. (2001). Adiabatically cured, alkali-activated cement-based wasteforms containing high levels of fly ash: formation of zeolites and Al-substituted CSH. *Cement Concrete Res.* 31, 1437–1447. doi: 10.1016/S0008-8846(01)00589-0

Buchwald, A., Hilbig, H., and Kaps, C. (2007). Alkali-activated metakaolin-slag blends—performance and structure in dependence of their composition. *J. Mater. Sci.* 42, 3024–3032. doi: 10.1007/s10853-006-0525-6

Buchwald, A., Zellmann, H.-D., and Kaps, C. (2011). Condensation of aluminosilicate gels—model system for geopolymer binders. *J. Non-Cryst. Solids.* 357 1376–1382. doi: 10.1016/j.jnoncrysol.2010.12.036

Cao, D., Su, D., Lu, B., and Yang, Y. (2005). Synthesis and structure characterisation of geopolymeric material based on metakaolin and phosphoric acid. *Guisuanyan Xuebao (J. Chin. Ceram. Soc.)* 33, 1385–1389.

Chancey, R. T., Stutzman, P., Juenger, M. C., and Fowler, D. W. (2010). Comprehensive phase characterization of crystalline and amorphous phases of a class F fly ash. *Cement Concrete Res.* 40, 146–156. doi: 10.1016/j.cemconres.2009.08.029

Chauhan, C., Vyas, P., and Joshi, M. (2011). Growth and characterization of Struvite-K crystals. *Cryst. Res. Technol.* 46, 187–194. doi: 10.1002/crat.201000587

Chauhan, C. K., Joseph, K., Parekh, B., and Joshi, M. (2008). Growth and characterization of struvite crystals. *Ind. J. Pure Appl. Phys.* 46, 507–512. Available online at: http://nopr.niscair.res.in/handle/123456789/1897 (accessed April 29, 2019).

Chauhan, C. K., and Joshi, M. J. (2014). Growth and characterization of struvite-Na crystals. *J. Cryst. Growth.* 401 221–226. doi: 10.1016/j.jcrysgro.2014.01.052

Chia, H. N., and Wu, B. M. (2015). Recent advances in 3D printing of biomaterials. *J. Biol. Eng.* 9:4. doi: 10.1186/s13036-015-0001-4

Chindaprasirt, P., De Silva, P., Sagoe-Crentsil, K., and Hanjitsuwan, S. (2012). Effect of SiO_2 and Al_2O_3 on the setting and hardening of high calcium fly ash-based geopolymer systems. *J. Mater. Sci.* 47, 4876–4883. doi: 10.1007/s10853-012-6353-y

Chindaprasirt, P., Rattanasak, U., and Taebuanhuad, S. (2013a). Role of microwave radiation in curing the fly ash geopolymer. *Adv. Powder Technol.* 24, 703–707. doi: 10.1016/j.apt.2012.12.005

Chindaprasirt, P., Thaiwitcharoen, S., Kaewpirom, S., and Rattanasak, U. (2013b). Controlling ettringite formation in FBC fly ash geopolymer concrete. *Cement Concrete Compos.* 41, 24–28. doi: 10.1016/j.cemconcomp.2013.04.009

Criado, M., Fernández-Jiménez, A., Palomo, A., Sobrados, I., and Sanz, J. (2008). Effect of the SiO_2/Na_2O ratio on the alkali activation of fly ash. Part II: 29Si MAS-NMR Survey. *Microporous Mesoporous Mater.* 109, 525–534. doi: 10.1016/j.micromeso.2007.05.062

Cui, X. M., Liu, L. P., He, Y., Chen, J. Y., and Zhou, J. (2011). A novel aluminosilicate geopolymer material with low dielectric loss. *Mater. Chem. Phys.* 130, 1–4. doi: 10.1016/j.matchemphys.2011.06.039

Cui, X. M., Zheng, G. J., Han, Y. C., Su, F., and Zhou, J. (2008). A study on electrical conductivity of chemosynthetic Al_2O_3-$2SiO_2$ geoploymer materials. *J. Power Sourc.* 184, 652–656. doi: 10.1016/j.jpowsour.2008.03.021

Davidovits, J. (2011). *Geopolymer Chemistry and Applications, 3rd Edn.* Saint-Quentin: Geopolymer Institute.

De Jong, B., Schramm, C. M., and Parziale, V. E. (1983). Polymerization of silicate and aluminate tetrahedra in glasses, melts, and aqueous solutions—IV. Aluminum coordination in glasses and aqueous solutions and comments on the aluminum avoidance principle. *Geochim. Cosmochim. Acta* 47, 1223–1236. doi: 10.1016/0016-7037(83)90064-9

De Rojas, M. S., and Frías, M. (1996). The pozzolanic activity of different materials, its influence on the hydration heat in mortars. *Cement Concrete Res.* 26, 203–213. doi: 10.1016/0008-8846(95)00200-6

Ding, Y., Dai, J. G., and Shi, C. J. (2016). Mechanical properties of alkali-activated concrete: A state-of-the-art review. *Constr. Build. Mater.* 127, 68–79. doi: 10.1016/j.conbuildmat.2016.09.121

Ding, Y., Dai, J. G., and Shi, C. J. (2018). Fracture properties of alkali-activated slag and ordinary Portland cement concrete and mortar. *Constr. Build. Mater.* 165, 310–320. doi: 10.1016/j.conbuildmat.2017.12.202

Ding, Z., Dong, B., Xing, F., Han, N., and Li, Z. (2012). Cementing mechanism of potassium phosphate based magnesium phosphate cement. *Ceram. Int.* 38, 6281–6288. doi: 10.1016/j.ceramint.2012.04.083

Douiri, H., Louati, S., Baklouti, S., Arous, M., and Fakhfakh, Z. (2014). Structural, thermal, and dielectric properties of phosphoric acid-based geopolymers with different amounts of H_3PO_4. *Mater. Lett.* 116, 9–12. doi: 10.1016/j.matlet.2013.10.075

Durdzinski, P. T., Dunant, C. F., Haha, M. B., and Scrivener, K. L. (2015). A new quantification method based on SEM-EDS to assess fly ash composition and study the reaction of its individual components in hydrating cement paste. *Cement Concrete Res.* 73, 111–122. doi: 10.1016/j.cemconres.2015.02.008

Duxson, P., Fernández-Jiménez, A., Provis, J. L., Lukey, G. C., Palomo, A., and van Deventer, J. S. J. (2006). Geopolymer technology: the current state of the art. *J. Mater. Sci.* 42, 2917–2933. doi: 10.1007/s10853-006-0637-z

Duxson, P., and Provis, J. L. (2008). Designing precursors for geopolymer cements. *J. Am. Ceram. Soc.* 91, 3864–3869. doi: 10.1111/j.1551-2916.2008.02787.x

Duxson, P., Provis, J. L., Lukey, G. C., and Van Deventer, J. S. (2007). The role of inorganic polymer technology in the development of 'green concrete'. *Cement Concrete Res.* 37, 1590–1597. doi: 10.1016/j.cemconres.2007.08.018

Fawer, M., Concannon, M., and Rieber, W. (1999). Life cycle inventories for the production of sodium silicates. *Int. J. Life Cycle Assess.* 4:207. doi: 10.1007/BF02979498

Feng, G., Cheng, P., Yan, W., Boronat, M., Li, X., Su, J. H., et al. (2016). Accelerated crystallization of zeolites via hydroxyl free radicals. *Science* 351, 1188–1191. doi: 10.1126/science.aaf1559

Fernández-Jiménez, A., Palomo, A., and Criado, M. (2005). Microstructure development of alkali-activated fly ash cement: a descriptive model. *Cement Concrete Res.* 35, 1204–1209. doi: 10.1016/j.cemconres.2004.08.021

Fernández-Jiménez, A., Palomo, A., Sobrados, I., and Sanz, J. (2006). The role played by the reactive alumina content in the alkaline activation of fly ashes. *Microporous Mesoporous Mater.* 91, 111–119. doi: 10.1016/j.micromeso.2005.11.015

Finch, T., and Sharp, J. H. (1989). Chemical reactions between magnesia and aluminium orthophosphate to form magnesia-phosphate cements. *J. Mater. Sci.* 24, 4379–4386. doi: 10.1007/BF00544516

Garcia-Lodeiro, I., Palomo, A., and Fernández-Jiménez, A. (2015). "An overview of the chemistry of alkali-activated cement-based binders," in *Handbook of Alkali-Activated Cements, Mortars and Concretes*, eds F. Pacheco-Torgal, J. Labrincha, C. Leonelli, A. Palomo, and P. Chindaprasit (Cambridge, UK: Elsevier), 19–47. doi: 10.1533/9781782422884.1.19

Gardner, L. J., Bernal, S. A., Walling, S. A., Corkhill, C. L., Provis, J. L., and Hyatt, N. C. (2015). Characterisation of magnesium potassium phosphate cements blended with fly ash and ground granulated blast furnace slag. *Cement Concrete Res.* 74, 78–87. doi: 10.1016/j.cemconres.2015.01.015

Giocondi, J. L., El-Dasher, B. S., Nancollas, G. H., and Orme, C. A. (2010). Molecular mechanisms of crystallization impacting calcium phosphate cements. *Philos. Trans. A Math. Phys. Eng. Sci.* 368, 1937–1961. doi: 10.1098/rsta.2010.0006

Guerrieri, M., and Sanjayan, J. G. (2010). Behavior of combined fly ash/slag-based geopolymers when exposed to high temperatures. *Fire Mater. Int. J.* 34, 163–175. doi: 10.1002/fam.1014

Guo, C. M., Wang, K. T., Liu, M. Y., Li, X. H., and Cui, X. M. (2016). Preparation and characterization of acid-based geopolymer using metakaolin and disused polishing liquid. *Ceram. Int.* 42, 9287–9291. doi: 10.1016/j.ceramint.2016.02.073

Guvendiren, M., Molde, J., Soares, R. M., and Kohn, J. (2016). Designing biomaterials for 3D printing. *ACS Biomater. Sci. Eng.* 2, 1679–1693. doi: 10.1021/acsbiomaterials.6b00121

Habert, G., d'Espinose de Lacaillerie, J. B., and Roussel, N. (2011). An environmental evaluation of geopolymer based concrete production: reviewing current research trends. *J. Cleaner Prod.* 19, 1229–1238. doi: 10.1016/j.jclepro.2011.03.012

Habert, G., and Ouellet-Plamondon, C. (2016). Recent update on the environmental impact of geopolymers. *RILEM Technol. Lett.* 1, 17–23. doi: 10.21809/rilemtechlett.2016.6

Handoo, S., Agarwal, S., and Agarwal, S. (2002). Physicochemical, mineralogical, and morphological characteristics of concrete exposed to elevated temperatures. *Cement Concrete Res.* 32, 1009–1018. doi: 10.1016/S0008-8846(01)00736-0

He, Y., Cui, X. M., Liu, X. D., Wang, Y. P., Zhang, J., and Liu, K. (2013). Preparation of self-supporting NaA zeolite membranes using geopolymers. *J. Membr. Sci.* 447, 66–72. doi: 10.1016/j.memsci.2013.07.027

He, Y., Liu, L., He, L., and Cui, X. (2016). Characterization of chemosynthetic H_3PO_4-Al_2O_3-$2SiO_2$ geopolymers. *Ceram. Int.* 42, 10908–10912. doi: 10.1016/j.ceramint.2016.03.224

Hill, R., and Howard, C. (1987). Quantitative phase analysis from neutron powder diffraction data using the Rietveld method. *J. Appl. Crystal.* 20, 467–474. doi: 10.1107/S0021889887086199

Inzana, J. A., Olvera, D., Fuller, S. M., Kelly, J. P., Graeve, O. A., Schwarz, E. M., et al. (2014). 3D printing of composite calcium phosphate and collagen scaffolds for bone regeneration. *Biomaterials* 35, 4026–4034. doi: 10.1016/j.biomaterials.2014.01.064

Ismail, I., Bernal, S. A., Provis, J. L., San Nicolas, R., Hamdan, S., and van Deventer, J. S. J. (2014). Modification of phase evolution in alkali-activated blast furnace slag by the incorporation of fly ash. *Cement Concrete Compos.* 45, 125–135. doi: 10.1016/j.cemconcomp.2013.09.006

ISO (2006). *Environmental Management: Life Cycle Assessment; Principles and Framework*. Geneva: International Organization for Standardization.

Jelinski, L. W., Graedel, T. E., Laudise, R. A., McCall, D. W., and Patel, C. K. (1992). Industrial ecology: concepts and approaches. *Proc. Natl. Acad. Sci. U.S.A.* 89, 793–797. doi: 10.1073/pnas.89.3.793

Katsiki, A. (2019). Aluminosilicate phosphate cements–a critical review. *Adv. Appl. Ceram.* doi: 10.1080/17436753.2019.1572339. [Epub ahead of print].

Khabbouchi, M., Hosni, K., Mezni, M., Zanelli, C., Doggy, M., Dondi, M., et al. (2017). Interaction of metakaolin-phosphoric acid and their structural evolution at high temperature. *Appl. Clay Sci.* 146, 510–516. doi: 10.1016/j.clay.2017.07.006

Khale, D., and Chaudhary, R. (2007). Mechanism of geopolymerization and factors influencing its development: a review. *J. Mater. Sci.* 42, 729–746. doi: 10.1007/s10853-006-0401-4

Kingery, W. D. (1950). Fundamental study of phosphate bonding in refractories: I, literature review. *J. Am. Ceram. Soc.* 33, 239–241. doi: 10.1111/j.1151-2916.1950.tb14171.x

Kingery, W. D. (1952). Fundamental study of phosphate bonding in refractories: IV, mortars bonded with monoaluminum and monomagnesium phosphate. *J. Am. Ceram. Soc.* 35, 61–63. doi: 10.1111/j.1151-2916.1952.tb13069.x

Kongshaug, G. (1998). "Energy consumption and greenhouse gas emissions in fertilizer production," in *IFA Technical Conference* (Marrakech: I International Fertilizer Industry Association).

Krizan, D., and Zivanovic, B. (2002). Effects of dosage and modulus of water glass on early hydration of alkali–slag cements. *Cement Concrete Res.* 32, 1181–1188. doi: 10.1016/S0008-8846(01)00717-7

Kühl, H. (1908). *Slag Cement and Process of Making the Same.* US Patent. No. 900939.

Kumar, S., and Kumar, R. (2011). Mechanical activation of fly ash: Effect on reaction, structure and properties of resulting geopolymer. *Ceram. Int.* 37, 533–541. doi: 10.1016/j.ceramint.2010.09.038

Li, C., Sun, H., and Li, L. (2010). A review: the comparison between alkali-activated slag (Si+ Ca) and metakaolin (Si+ Al) cements. *Cement Concrete Res.* 40, 1341–1349. doi: 10.1016/j.cemconres.2010.03.020

Lim, S., Buswell, R. A., Le, T. T., Austin, S. A., Gibb, A. G. F., and Thorpe, T. (2012). Developments in construction-scale additive manufacturing processes. *Autom. Constr.* 21, 262–268. doi: 10.1016/j.autcon.2011.06.010

Liu, L. P., Cui, X. M., He, Y., Liu, S. D., and Gong, S. Y. (2012). The phase evolution of phosphoric acid-based geopolymers at elevated temperatures. *Mater. Lett.* 66, 10–12. doi: 10.1016/j.matlet.2011.08.043

Liu, L. P., Cui, X. M., Qiu, S. H., Yu, J. L., and Zhang, L. (2010). Preparation of phosphoric acid-based porous geopolymers. *Appl. Clay Sci.* 50, 600–603. doi: 10.1016/j.clay.2010.10.004

Lodeiro, I. G., Fernández-Jiménez, A., Palomo, A., and Macphee, D. E. (2010). Effect on fresh CSH gels of the simultaneous addition of alkali and aluminium. *Cement Concrete Res.* 40, 27–32. doi: 10.1016/j.cemconres.2009.08.004

Lothenbach, B., Scrivener, K., and Hooton, R. (2011). Supplementary cementitious materials. *Cement Concrete Res.* 41, 1244–1256. doi: 10.1016/j.cemconres.2010.12.001

Louati, S., Baklouti, S., and Samet, B., (2016). Acid based geopolymerization kinetics: effect of clay particle size. *Appl. Clay Sci.* 132–133, 571–578. doi: 10.1016/j.clay.2016.08.007

Louati, S., Hajjaji, W., Baklouti, S., and Samet, B., (2014). Structure and properties of new eco-material obtained by phosphoric acid attack of natural tunisian clay. *Appl. Clay Sci.* 101, 60–67. doi: 10.1016/j.clay.2014.07.015

Luna Galiano, Y., Fernández Pereira, C., and Vale, J. (2011). Stabilization/solidification of a municipal solid waste incineration residue using fly ash-based geopolymers. *J. Hazard. Mater.* 185, 373–381. doi: 10.1016/j.jhazmat.2010.08.127

Luukkonen, T., Heponiemi, A., Runtti, H., Pesonen, J., Yliniemi, J., and Lassi, U., (2019). Application of alkali-activated materials for water and wastewater treatment: a review. *Rev. Environ. Sci. BioTechnol.* doi: 10.1007/s11157-019-09494-0. [Epub ahead of print].

Luxán, M. P., Madruga, F., and Saavedra, J. (1989). Rapid evaluation of pozzolanic activity of natural products by conductivity measurement. *Cement Concrete Res.* 19, 63–68. doi: 10.1016/0008-8846(89)90066-5

Luz, A. P., Gomes, D. T., and Pandolfelli, V. C. (2015). High-alumina phosphate-bonded refractory castables: Al(OH)3 sources and their effects. *Ceram. Int.* 41, 9041–9050. doi: 10.1016/j.ceramint.2015.03.276

Ma, H., Xu, B., and Li, Z. (2014). Magnesium potassium phosphate cement paste: degree of reaction, porosity and pore structure. *Cement Concrete Res.* 65, 96–104. doi: 10.1016/j.cemconres.2014.07.012

MacKenzie, K. (2015). "Innovative applications of inorganic polymers (geopolymers)," in *Handbook of Alkali-Activated Cements, Mortars and Concretes*, eds F. Pacheco-Torgal, J. Labrincha, C. Leonelli, A. Palomo, and P. Chindaprasit (Cambridge, UK: Elsevier), 777–805. doi: 10.1533/9781782422884.5.777

Mackenzie, K. J., Brew, D., Fletcher, R., Nicholson, C. L., Vagana, R., and Schmucker, M. (2005). "Towards an understanding of the synthesis mechanisms of geopolymer materials," in *Proceedings of the World Geopolymer , Geopolymer Green Chemistry Sustainable Development Solutions* (Saint-Quentin), 41–44.

MacKenzie, K. J., Rahner, N., Smith, M. E., and Wong, A. (2010). Calcium-containing inorganic polymers as potential bioactive materials. *J. Mat. Sci.* 45:999. doi: 10.1007/s10853-009-4031-5

MacKenzie, K. J., Smith, M. E., Wong, A., Hanna, J. V., Barry, B., and Barsoum, M. W. (2011). Were the casing stones of Senefru's Bent Pyramid in Dahshour cast or carved?: multinuclear NMR evidence. *Mater. Lett.* 65, 350–352. doi: 10.1016/j.matlet.2010.10.035

Mathivet, V., Jouin, J., Gharzouni, A., Sobrados, I., Celerier, H., Rossignol, S., et al. (2019). Acid-based geopolymers: understanding of the structural evolutions during consolidation and after thermal treatments. *J. Non Cryst. Solids* 512, 90–97. doi: 10.1016/j.jnoncrysol.2019.02.025

Morrissey, A. J., and Browne, J. (2004). Waste management models and their application to sustainable waste management. *Waste Manage.* 24, 297–308. doi: 10.1016/j.wasman.2003.09.005

Najafi Kani, E., Allahverdi, A., and Provis, J. L. (2012). Efflorescence control in geopolymer binders based on natural pozzolan. *Cement Concrete Compos.* 34, 25–33. doi: 10.1016/j.cemconcomp.2011.07.007

Nath, S., and Kumar, S. (2013). Influence of iron making slags on strength and microstructure of fly ash geopolymer. *Constr. Build. Mater.* 38, 924–930. doi: 10.1016/j.conbuildmat.2012.09.070

Nazari, A., Bagheri, A., and Riahi, S. (2011). Properties of geopolymer with seeded fly ash and rice husk bark ash. *Mater. Sci. Eng. A* 528, 7395–7401. doi: 10.1016/j.msea.2011.06.027

Nematollahi, B., and Sanjayan, J. (2014). Effect of different superplasticizers and activator combinations on workability and strength of fly ash based geopolymer. *Mater. Des.* 57, 667–672. doi: 10.1016/j.matdes.2014.01.064

Neville, A. M. (2011). *Properties of Concrete, 4th Edn.* London: Pearson Education Limited.

Nicholson, C. L., Murray, B. J., Fletcher, R. A., Brew, D., Mackenzie, K. J., and Schmücker, M. (2005). "Novel geopolymer materials containing borate structural units," in *World Congress Geopolymer* (Saint-Quentin), 31–33.

Ouellet-Plamondon, C., and Habert, G. (2015). "Life cycle assessment (LCA) of alkali-activated cements and concretes," in *Handbook of Alkali-Activated Cements, Mortars and Concretes*, eds F. Pacheco-Torgal, J. Labrincha, C. Leonelli, A. Palomo, and P. Chindaprasit (Cambridge, UK: Elsevier), 663–686. doi: 10.1533/9781782422884.5.663

Pacheco-Torgal, F. (2015). "Introduction to handbook of alkali-activated cements, mortars and concretes," in *Handbook of Alkali-Activated Cements, Mortars and Concretes*, eds F. Pacheco-Torgal, J. Labrincha, C. Leonelli, A. Palomo, and P. Chindaprasit (Cambridge, UK: Elsevier), 1–16. doi: 10.1533/9781782422884.1

Pacheco-Torgal, F., Castro-Gomes, J., and Jalali, S. (2008). Alkali-activated binders: a review - Part 1. Historical background, terminology, reaction mechanisms and hydration products. *Construct. Build. Mater.* 22, 1305–1314. doi: 10.1016/j.conbuildmat.2007.10.015

Passuello, A., Rodriguez, E. D., Hirt, E., Longhi, M., Bernal, S. A., Provis, J. L., et al. (2017). Evaluation of the potential improvement in the environmental footprint of geopolymers using waste-derived activators. *J. Clean. Prod.* 166, 680–689. doi: 10.1016/j.jclepro.2017.08.007

Perera, D. S., Hanna, J. V., Davis, J., Blackford, M. G., Latella, B. A., Sasaki, Y., et al. (2008). Relative strengths of phosphoric acid-reacted and alkali-reacted metakaolin materials. *J.Mater. Sci.* 43, 6562–6566. doi: 10.1007/s10853-008-2913-6

Provis, J. L. (2013). Geopolymers and other alkali activated materials: why, how, and what? *Mater. Struct.* 47, 11–25. doi: 10.1617/s11527-013-0211-5

Provis, J. L., and Bernal, S. A. (2014). Geopolymers and related alkali-activated materials. *Annu. Rev. Mater. Res.* 44, 299–327. doi: 10.1146/annurev-matsci-070813-113515

Provis, J. L., Palomo, A., and Shi, C. (2015). Advances in understanding alkali-activated materials. *Cement Concrete Res.* 78, 110–125. doi: 10.1016/j.cemconres.2015.04.013

Provis, J. L., and Van Deventer, J. S. (2013). *Alkali Activated Materials: State-of-the-Art Report, RILEM TC 224-AAM.* Dordrecht: Springer Science Business Media. doi: 10.1007/978-94-007-7672-2

Rao, F., and Liu, Q. (2015). Geopolymerization and its potential application in mine tailings consolidation: a review. *Miner. Process. Extract. Metall. Rev.* 36, 399–409. doi: 10.1080/08827508.2015.1055625

Rashad, A. M., Zeedan, S. R., and Hassan, H. A. (2012). A preliminary study of autoclaved alkali-activated slag blended with quartz powder. *Construct. Build. Mater.* 33, 70–77. doi: 10.1016/j.conbuildmat.2011.12.104

Raven, K., and Loeppert, R. (1996). Microwave digestion of fertilizers and soil amendments. *Commun. Soil Sci. Plant Anal.* 27, 2947–2971. doi: 10.1080/00103629609369754

Reddy, M. S., Dinakar, P., and Rao, B. H. (2016). A review of the influence of source material's oxide composition on the compressive

strength of geopolymer concrete. *Microporous Mesoporous Mater.* 234, 12–23. doi: 10.1016/j.micromeso.2016.07.005

Rengier, F., Mehndiratta, A., Von Tengg-Kobligk, H., Zechmann, C. M., Unterhinninghofen, R., Kauczor, H. U., et al. (2010). 3D printing based on imaging data: review of medical applications. *Int. J. Comput. Assist. Radiol. Surg.* 5, 335–341. doi: 10.1007/s11548-010-0476-x

Richardson, I., Brough, A., Groves, G., and Dobson, C. (1994). The characterization of hardened alkali-activated blast-furnace slag pastes and the nature of the calcium silicate hydrate (CSH) phase. *Cement Concrete Res.* 24, 813–829. doi: 10.1016/0008-8846(94)90002-7

Richardson, I. G., Brough, A. R., Brydson, R., Groves, G. W., and Dobson, C. M. (1993). Location of aluminum in substituted calcium silicate hydrate (C-S-H) gels as determined by 29Si and 27Al NMR and EELS. *J. Am. Ceram. Soc.* 76, 2285–2288. doi: 10.1111/j.1151-2916.1993.tb07765.x

Roy, D. M. (1987). New strong cement materials: chemically bonded ceramics. *Science* 235, 651–658. doi: 10.1126/science.235.4789.651

Saxena, S., and D'Souza, S. (2006). Heavy metal pollution abatement using rock phosphate mineral. *Environ. Int.* 32, 199–202. doi: 10.1016/j.envint.2005.08.011$$$

Scarlett, N. V. Y., and Madsen, I. C. (2012). Quantification of phases with partial or no known crystal structures. *Powder Diffract.* 21, 278–284. doi: 10.1154/1.2362855

Shang, J., Dai, J. G., Zhao, T. J., Guo, S. Y., Zhang, P., and Mu, B. (2018). Alternation of traditional cement mortars using fly ash-based geopolymer mortars modified by slag. *J. Clean. Prod.* 203, 746–756. doi: 10.1016/j.jclepro.2018.08.255

Shi, C., Jiménez, A. F., and Palomo, A. (2011). New cements for the 21st century: the pursuit of an alternative to Portland cement. *Cement Concrete Res.* 41, 750–763. doi: 10.1016/j.cemconres.2011.03.016

Shi, C., and Qian, J. (2000). High performance cementing materials from industrial slags-a review. *Resour. Conserv. Recycl.* 29, 195–207. doi: 10.1016/S0921-3449(99)00060-9

Škvára, F., Kopecký, L., Myšková, L., Šmilauer, V., Alberovská, L., and Vinšová, L. (2009). Aluminosilicate polymers-influence of elevated temperatures, efflorescence. *Ceram.-Silikáty* 53, 276–282. Available online at: http://www.ceramics-silikaty.cz/2009/pdf/2009_04_276.pdf (accessed April 29, 2019).

Sperinck, S., Raiteri, P., Marks, N., and Wright, K. (2011). Dehydroxylation of kaolinite to metakaolin-a molecular dynamics study. *J. Mater. Chem.* 21, 2118–2125. doi: 10.1039/C0JM01748E

Tailby, J., and MacKenzie, K. J. (2010). Structure and mechanical properties of aluminosilicate geopolymer composites with Portland cement and its constituent minerals. *Cement Concrete Res.* 40, 787–794. doi: 10.1016/j.cemconres.2009.12.003

Tamimi, F., Sheikh, Z., and Barralet, J. (2012). Dicalcium phosphate cements: brushite and monetite. *Acta Biomater.* 8, 474–487. doi: 10.1016/j.actbio.2011.08.005

Taylor, H. F. (1997). *Cement Chemistry.* New York, NY: Thomas Telford. doi: 10.1680/cc.25929

Temuujin, J., Minjigmaa, A., Davaabal, B., Bayarzul, U., Ankhtuya, A., Jadambaa, T., et al. (2014). Utilization of radioactive high-calcium Mongolian flyash for the preparation of alkali-activated geopolymers for safe use as construction materials. *Ceram. Int.* 40, 16475–16483. doi: 10.1016/j.ceramint.2014.07.157

Toniolo, N., and Boccaccini, A. R. (2017). Fly ash-based geopolymers containing added silicate waste. A review. *Ceram. Int.* 43, 14545–14551. doi: 10.1016/j.ceramint.2017.07.221

Utneja, S., Nawal, R. R., Talwar, S., and Verma, M. (2015). Current perspectives of bio-ceramic technology in endodontics: calcium enriched mixture cement-review of its composition, properties and applications. *Restor. Dent. Endod.* 40, 1–13. doi: 10.5395/rde.2015.40.1.1

Van Jaarsveld, J., Van Deventer, J., and Lorenzen, L. (1997). The potential use of geopolymeric materials to immobilise toxic metals. *Miner. Eng.* 10, 659–669. doi: 10.1016/S0892-6875(97)00046-0

Vassilev, S. V., and Vassileva, C. G. (2005). Methods for characterization of composition of fly ashes from coal-fired power stations: a critical overview. *Energy Fuels* 19, 1084–1098. doi: 10.1021/ef049694d

Wagh, A. S. (2004). "Chemically bonded phosphate ceramics-a novel class of geopolymers," in *Advances in Ceramic Matrix Composites X: Proceedings of the 106th Annual Meeting of the American Ceramic Society* (Indianapolis, IN), 107. doi: 10.1002/9781118408353.ch10

Wagh, A. S. (2016). *Chemically Bonded Phosphate Ceramics: Twenty-First Century Materials With Diverse Applications.* Oxford, UK: Elsevier. doi: 10.1016/B978-0-08-100380-0.00002-6

Wagh, A. S., and Jeong, S. Y. (2003a). Chemically bonded phosphate ceramics: I, a dissolution model of formation. *J. Am. Ceram. Soc.* 86, 1838–1844. doi: 10.1111/j.1151-2916.2003.tb03569.x

Wagh, A. S., and Jeong, S. Y. (2003b). Chemically bonded phosphate ceramics: III, reduction mechanism and its application to iron phosphate ceramics. *J. Am. Ceram. Soc.* 86, 1850–1855. doi: 10.1111/j.1151-2916.2003.tb03571.x

Walkley, B., Nicolas, R. S., Sani, M. A., Bernal, S. A., van Deventer, J. S. J., and Provis, J. L. (2017). Structural evolution of synthetic alkali-activated CaO-MgO-Na2O-Al2O3-SiO2 materials is influenced by Mg content. *Cement Concrete Res.* 99, 155–171. doi: 10.1016/j.cemconres.2017.05.006

Walling, S. A., and Provis, J. L. (2016). Magnesia-based cements: a journey of 150 years, and cements for the future? *Chem. Rev.* 116, 4170–4204. doi: 10.1021/acs.chemrev.5b00463

Wang, S. D., and Scrivener, K. L. (1995). Hydration products of alkali activated slag cement. *Cement Concrete Res.* 25, 561–571. doi: 10.1016/0008-8846(95)00045-E

Wang, S. D., Scrivener, K. L., and Pratt, P. (1994). Factors affecting the strength of alkali-activated slag. *Cement Concrete Res.* 24, 1033–1043. doi: 10.1016/0008-8846(94)90026-4

Wang, W. C., Wang, H.-Y., and Tsai, H.-C. (2016). Study on engineering properties of alkali-activated ladle furnace slag geopolymer. *Constr. Build. Mater.* 123, 800–805. doi: 10.1016/j.conbuildmat.2016.07.068

Wang, Y. S. (2018). *Influence of Metal Ions on Formation of Silico-Aluminophosphate Geopolymer.* Kowloon: The Hong Kong Polytechnic University.

Wang, Y. S., and Dai, J. G. (2017). Use of magnesia sand for optimal design of high performance magnesium potassium phosphate cement mortar. *Constr. Build. Mater.* 153, 385–392. doi: 10.1016/j.conbuildmat.2017.07.099

Wang, Y. S., Dai, J. G., Ding, Z., and Xu, W.-T. (2017). Phosphate-based geopolymer: formation mechanism and thermal stability. *Mater. Lett.* 190, 209–212. doi: 10.1016/j.matlet.2017.01.022

Wang, Y. S., Dai, J. G., Wang, L., Tsang, D. C. W., and Poon, C. S. (2018a). Influence of lead on stabilization/solidification by ordinary Portland cement and magnesium phosphate cement. *Chemosphere* 190, 90–96. doi: 10.1016/j.chemosphere.2017.09.114

Wang, Y. S., Provis, J. L., and Dai, J. G. (2018b). Role of soluble aluminum species in the activating solution for synthesis of silico-aluminophosphate geopolymers. *Cement Concrete Compos.* 93, 186–195. doi: 10.1016/j.cemconcomp.2018.07.011

Wilson, A. D., and Nicholson, J. W. (2005). *Acid-base Cements: Their Biomedical and Industrial Applications.* Cambridge, UK: Cambridge University Press.

Wood, S., and Cowie, A. (2004). *A Review of Greenhouse Gas Emission Factors for Fertiliser Production.* IEA Bioenergy Task.

Xia, M., and Sanjayan, J. (2016). Method of formulating geopolymer for 3D printing for construction applications. *Mater. Des.* 110, 382–390. doi: 10.1016/j.matdes.2016.07.136

Xu, G., and Shi, X. (2018). Characteristics and applications of fly ash as a sustainable construction material: a state-of-the-art review. *Resour. Conserv. Recycl.* 136, 95–109. doi: 10.1016/j.resconrec.2018.04.010

Xu, G., Zhong, J., and Shi, X. (2018). Influence of graphene oxide in a chemically activated fly ash. *Fuel* 226, 644–657. doi: 10.1016/j.fuel.2018.04.033

Xu, H., Van Deventer, J., and Lukey, G. (2001). Effect of alkali metals on the preferential geopolymerization of stilbite/kaolinite mixtures. *Ind. Eng. Chem. Res.* 40, 3749–3756. doi: 10.1021/ie010042b

Xu, H. H., and Simon, C. G. Jr. (2005). Fast setting calcium phosphate-chitosan scaffold: mechanical properties and biocompatibility. *Biomaterials* 26, 1337–1348. doi: 10.1016/j.biomaterials.2004.04.043

Xu, W., Dai, J.-G., Ding, Z., and Wang, Y. (2017). Polyphosphate-modified calcium aluminate cement under normal and elevated temperatures: Phase evolution, microstructure, and mechanical properties. *Ceram. Int.* 43, 15525–15536. doi: 10.1016/j.ceramint.2017.08.102

Xue, X., Liu, Y. L., Dai, J. G., Poon, C. S., Zhang, W. D., and Zhang, P. (2018). Inhibiting efflorescence formation on fly ash-based geopolymer via silane surface modification. *Cement Concrete Compos.* 94, 43–52. doi: 10.1016/j.cemconcomp.2018.08.013

Xue, Z., Zhang, H., Jin, A., Ye, J., Ren, L., Ao, J., et al. (2012). Correlation between degradation and compressive strength of an injectable macroporous calcium phosphate cement. *J. Alloys Compd.* 520, 220–225. doi: 10.1016/j.jallcom.2012.01.022

Yao, Z. T., Ji, X. S., Sarker, P. K., Tang, J. H., Ge, L. Q., Xia, M. S., et al. (2015). A comprehensive review on the applications of coal fly ash. *Earth-Sci. Rev.* 141, 105–121. doi: 10.1016/j.earscirev.2014.11.016

Zhang, J., Liu, W., Schnitzler, V., Tancret, F., and Bouler, J. M. (2014). Calcium phosphate cements for bone substitution: chemistry, handling and mechanical properties. *Acta Biomater.* 10, 1035–1049. doi: 10.1016/j.actbio.2013.11.001

Zhang, Z., Provis, J. L., Reid, A., and Wang, H. (2014). Fly ash-based geopolymers: the relationship between composition, pore structure and efflorescence. *Cement Concrete Res.* 64, 30–41. doi: 10.1016/j.cemconres.2014.06.004

Zhang, Z., Provis, J. L., Zou, J., Reid, A., and Wang, H. (2016). Toward an indexing approach to evaluate fly ashes for geopolymer manufacture. *Cement Concrete Res.* 85, 163–173. doi: 10.1016/j.cemconres.2016.04.007

Zhong, J., Zhou, G. X., He, P. G., Yang, Z. H., and Jia, D. C. (2017). 3D printing strong and conductive geo-polymer nanocomposite structures modified by graphene oxide. *Carbon* 117, 421–426. doi: 10.1016/j.carbon.2017.02.102